Article

Current Biology

A GH81-type β-glucan-binding protein enhances colonization by mutualistic fungi in barley

Graphical abstract

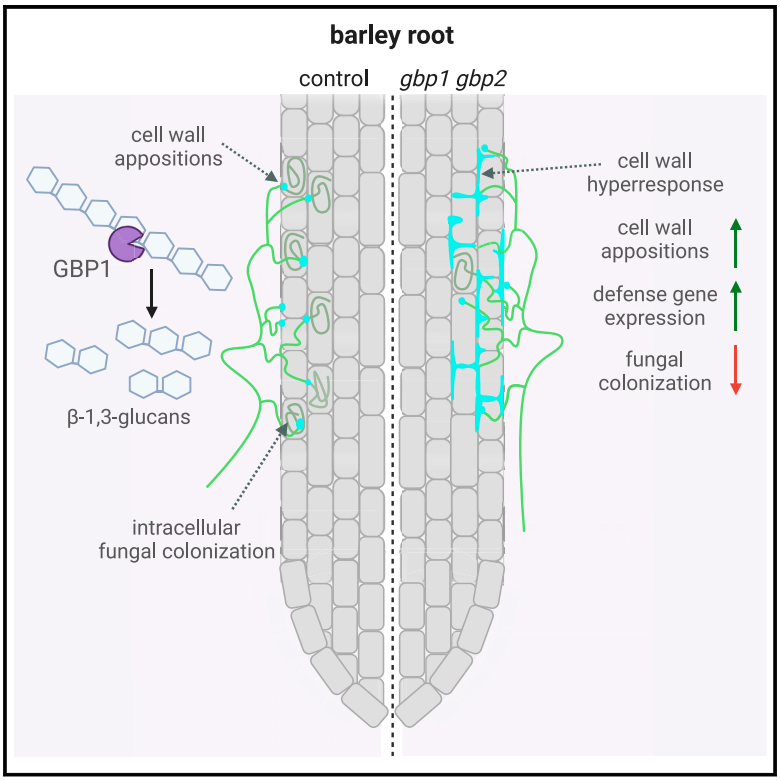

Authors

Alan Wanke, Sarah van Boerdonk, Lisa Katharina Mahdi, ..., Ivan F. Acosta, Cyril Zipfel, Alga Zuccaro

Correspondence

azuccaro@uni-koeln.de

In brief

Wanke et al. identify GBP1, a family 81 glycoside hydrolase, as a β-glucan interactor in barley. Mutating both barley *GBP* paralogs reduces colonization by beneficial root endophytes, arbuscular mycorrhizal fungi, and pathogens. These findings provide insights into the role of β-1,3-glucanases as compatibility factors in plant-fungal interactions.

Highlights

- Barley GBP1 is a β-1,3-endoglucanase
- GBPs contribute to the establishment of symbiotic associations in barley
- Upon fungal colonization, *gbp* mutants display enhanced cell wall immune responses
- Barley *GBP* mutation increases resistance to pathogen infection in roots and leaves

Wanke et al., 2023, Current Biology *33*, 5071–5084
December 4, 2023
https://doi.org/10.1016/j.cub.2023.10.048

CellPress

Current Biology

CellPress
OPEN ACCESS

Article

A GH81-type β-glucan-binding protein enhances colonization by mutualistic fungi in barley

Alan Wanke,[1,2,8] Sarah van Boerdonk,[1,2] Lisa Katharina Mahdi,[1,2] Stephan Wawra,[1] Miriam Neidert,[1] Balakumaran Chandrasekar,[1,6,9] Pia Saake,[1,6] Isabel M.L. Saur,[1,6] Paul Derbyshire,[3] Nicholas Holton,[3] Frank L.H. Menke,[3] Mathias Brands,[1] Markus Pauly,[4,7] Ivan F. Acosta,[2] Cyril Zipfel,[3,5] and Alga Zuccaro[1,6,10,*]

[1]Institute for Plant Sciences, University of Cologne, Cologne, Germany
[2]Max Planck Institute for Plant Breeding Research, Cologne, Germany
[3]The Sainsbury Laboratory, University of East Anglia, Norwich, UK
[4]Institute of Plant Cell Biology and Biotechnology, Heinrich-Heine University Düsseldorf, Düsseldorf, Germany
[5]Institute of Plant and Microbial Biology, University of Zurich, and Zurich-Basel Plant Science Center, Zurich, Switzerland
[6]Cluster of Excellence on Plant Sciences (CEPLAS), Cologne, Germany
[7]Cluster of Excellence on Plant Sciences (CEPLAS), Düsseldorf, Germany
[8]Present address: Sainsbury Laboratory, University of Cambridge, Cambridge, UK
[9]Present address: Department of Biological Sciences, Birla Institute of Technology & Science, Pilani (BITS Pilani), Pilani, India
[10]Lead contact
*Correspondence: azuccaro@uni-koeln.de
https://doi.org/10.1016/j.cub.2023.10.048

SUMMARY

Cell walls are important interfaces of plant-fungal interactions, acting as robust physical and chemical barriers against invaders. Upon fungal colonization, plants deposit phenolics and callose at the sites of fungal penetration to prevent further fungal progression. Alterations in the composition of plant cell walls significantly impact host susceptibility. Furthermore, plants and fungi secrete glycan hydrolases acting on each other's cell walls. These enzymes release various sugar oligomers into the apoplast, some of which activate host immunity via surface receptors. Recent characterization of cell walls from plant-colonizing fungi has emphasized the abundance of β-glucans in different cell wall layers, which makes them suitable targets for recognition. To characterize host components involved in immunity against fungi, we performed a protein pull-down with the biotinylated β-glucan laminarin. Thereby, we identified a plant glycoside hydrolase family 81-type glucan-binding protein (GBP) as a β-glucan interactor. Mutation of *GBP1* and its only paralog, *GBP2*, in barley led to decreased colonization by the beneficial root endophytes *Serendipita indica* and *S. vermifera*, as well as the arbuscular mycorrhizal fungus *Rhizophagus irregularis*. The reduction of colonization was accompanied by enhanced responses at the host cell wall, including an extension of callose-containing cell wall appositions. Moreover, *GBP* mutation in barley also reduced fungal biomass in roots by the hemibiotrophic pathogen *Bipolaris sorokiniana* and inhibited the penetration success of the obligate biotrophic leaf pathogen *Blumeria hordei*. These results indicate that GBP1 is involved in the establishment of symbiotic associations with beneficial fungi—a role that has potentially been appropriated by barley-adapted pathogens.

INTRODUCTION

Cell walls (CWs) are key interfaces in plant-fungal interactions, representing the first point of physical contact between the invading fungus and its potential host. Plant CWs consist of adaptable networks of cellulose microfibrils embedded in a matrix of hemicellulose (mostly xyloglucan, mannan, and xylans), pectins, and hydrophobic polymers such as cutin, lignin, and suberin. Their architecture and composition are highly responsive to external and internal cues.[1,2] Plant CWs act as scaffolds for hydrolytic enzymes and reservoirs for antimicrobial substances such as secondary metabolites and reactive oxygen species (ROS).[3–6] To gain access to the nutritional resources of the host, fungi need to bypass these chemical and physical barriers. They do so by employing either carbohydrate active enzymes (CAZymes) and/or specialized pressure-driven penetration structures like appressoria. Plants counteract those strategies by forming carbohydrate-enriched CW appositions (CWAs), so-called papillae, which act as CW reinforcements at the sites of fungal penetrations.[7] Although the relevance of papillae in preventing or delaying fungal colonization has been controversial in recent decades, many studies correlated the effectiveness of papillae to the timing of deposition, size, architecture, and composition of the papillae.[3,8,9] Systematic screenings of *Arabidopsis thaliana* CW mutants have shown that interference with the structure and composition of plant CWs severely impacts fungal compatibility.[10] Besides the direct effects of changes in CW architecture, compromised CW integrity can indirectly prime host defenses and/or alter phytohormone levels, ultimately impacting the success of fungal colonization.[10–14]

Both fungi and plants secrete a plethora of CAZymes upon confrontation. These host and fungal hydrolases not only physically damage each other's CWs but also release carbohydrate oligomers as degradation products that can inform the host's immune system about the invading microbe. Fungal chitin and its deacetylated derivative chitosan are well-studied microbe-associated molecular patterns (MAMPs) that—upon perception by cell surface receptors—mount a range of defense responses such as the production of ROS and the secretion of antimicrobials.[15,16] Furthermore, fungal hydrolases and mechanical forces exerted during fungal penetration release a variety of plant CW-derived fragments, functioning as damage-associated molecular patterns (DAMPs).[17] This recognition of ''modified self'' similarly initiates immune signaling pathways. Examples for unequivocal plant CW-derived DAMPs are cellulose oligomers, pectin oligogalacturonides, as well as mannan, xyloglucan, and arabinoxylan fragments.[18–25]

In the context of fungal colonization, β-glucans can either enhance or suppress immune responses, depending on their structure and branch decorations, and cannot be clearly categorized as MAMPs or DAMPs. They represent the major component of most fungal cell surface glycans, being part of both the outer layer of the rigid fungal CW as well as the surrounding gel-like extracellular polysaccharide (EPS) matrix loosely attached to the CW.[26,27] Plants secrete various carbohydrate hydrolases, among them β-glucanases, that target these fungal glycans.[28,29] The potential of some glycans to act as MAMPs and elicit pattern-triggered immunity has been demonstrated for a wide range of host plants.[30] Notably, plants respond differentially to short-chain and long-chain β-1,3-glucans.[31] Although *Arabidopsis thaliana* Col-0 mounts immune responses such as ROS production, cytosolic calcium influx, mitogen-activated protein kinase (MAPK) activation, and pathogenesis-related (PR) gene expression induction upon treatment with short-chain β-1,3-glucans like laminarihexaose, it does not respond to long-chain β-1,3-glucans. By contrast, immune responses in *Nicotiana benthamiana* are only activated upon treatment with long-chain β-1,3-glucans. The monocots *Hordeum vulgare* (barley) and *Brachypodium distachyon* are able to perceive both types of β-1,3-glucan independent of their degree of polymerization.[31,32] Although the responses to laminarihexaose in Arabidopsis are mediated by the central carbohydrate-binding lysin motif (LysM) receptor kinase CERK1, perception of long-chain β-1,3-glucans in *N. benthamiana* and *Oryza sativa* is CERK1-independent.[31,32] It was recently suggested that β-glucan oligomers from fungal cell surface glycans do not function exclusively as MAMPs. Upon fungal colonization, barley secretes the β-1,3-glucanase BGLUII (apoplastic glycoside hydrolase 17 family, GH17), which releases a highly substituted and specific β-1,3-glucan decasaccharide (β-GD) from the fungal EPS matrix.[33] Instead of activating immune responses in its host, β-GD exhibits antioxidative properties that helps the fungus to overcome the hostile oxidative environment and, thereby, facilitate host colonization. In addition to their occurrence in fungal CWs, β-1,3-glucan polymers are major components of callose in host CWAs.[7] Since the release of callose fragments from papillae by mechanical force or enzymatic digest is conceivable, β-1,3-glucan oligomers can serve a dual function as DAMPs and/or MAMPs.[32,34] A similar dual role has been recently attributed to immunogenic mixed-linked β-1,3/1,4-glucans that can be found in the CWs of grasses as well as fungi and other microbes.[35,36]

To detect novel components linked to β-glucan signaling in barley, we performed a protein pull-down with biotinylated laminarin, a β-1,6-branched β-1,3-glucan also found in fungal CWs. Thereby, we identified the GH81 β-1,3-endoglucanase GBP1 as an interactor of β-1,3/1,6-glucans. Purified GBP1 specifically hydrolyzes β-1,3-linked glucans and can modulate ROS production in *N. benthamiana* and *H. vulgare*. CRISPR-Cas9-generated mutation of the two *GBP* gene copies in barley decreased the colonization efficiency of the beneficial root endophytes *Serendipita indica* and *Serendipita vermifera* (Basidiomycota) as well as the arbuscular mycorrhizal (AM) fungus *Rhizophagus irregularis* (Glomeromycotina). This phenotype was accompanied by a hyper-response of the host CW during fungal colonization. Additionally, *gbp* double mutants were more resistant to root infection with the hemibiotrophic pathogen *Bipolaris sorokiniana* and penetration success of the leaf pathogen *Blumeria hordei* (Ascomycota) was reduced at 48 h post infection. Altogether, this suggests a previously undescribed role of β-1,3-endoglucanases as tissue-independent broad-range compatibility factors for fungal colonization.

RESULTS

Barley GBP-type enzymes mediate compatibility to leaf and root colonization by fungi with different lifestyles

Leaf and root tissues of barley express the cellular machinery necessary to sense the long-chain β-1,3/β-1,6 branched glucan laminarin and to mount immune responses such as the production of apoplastic ROS[31] (Figure S1A). To discover interactors of long-chain β-glucans, we performed a protein pull-down using biotinylated laminarin as bait. The biotinylated and non-biotinylated versions of laminarin induced similar ROS burst responses in barley (Figure S1B), confirming that biotinylation of laminarin does not alter its immunogenic potential. Non-biotinylated laminarin and biotinylated elf18 were included as control treatments. Elf18 is a peptide derived from the prokaryotic elongation factor Tu, a well-characterized immunogenic peptide solely perceived by *Brassicaceae* members.[37,38] Eluted proteins were separated by SDS-PAGE (Figure S1C), extracted from the gel, and further subjected to tandem mass spectrometric analysis. A total of 101 proteins were identified across the three treatments, based on strict criteria for candidate selection (i.e., proteins detected in three out of four replicates) (Table S1). Although the majority of these proteins were shared across all three treatments (96 proteins), the only interactor detected exclusively after biotinylated laminarin treatment (Figure 1A) was the β-glucan-binding protein GBP1 (HORVU5Hr1G059430.56). Despite the absence of a predicted signal peptide in its gene sequence, GBP1 was previously identified in barley apoplastic fluids following colonization by the mutualistic root endophyte *S. indica*.[39] In support of this, another study demonstrates that a GBP ortholog in soybean is secreted into the apoplastic space even in the absence of a signal peptide.[40] GBPs are found in the genomes of most land plants, including bryophytes, ferns, and angiosperms. They have been duplicated several times throughout the evolution of plants, with a large expansion in legumes. Barley has

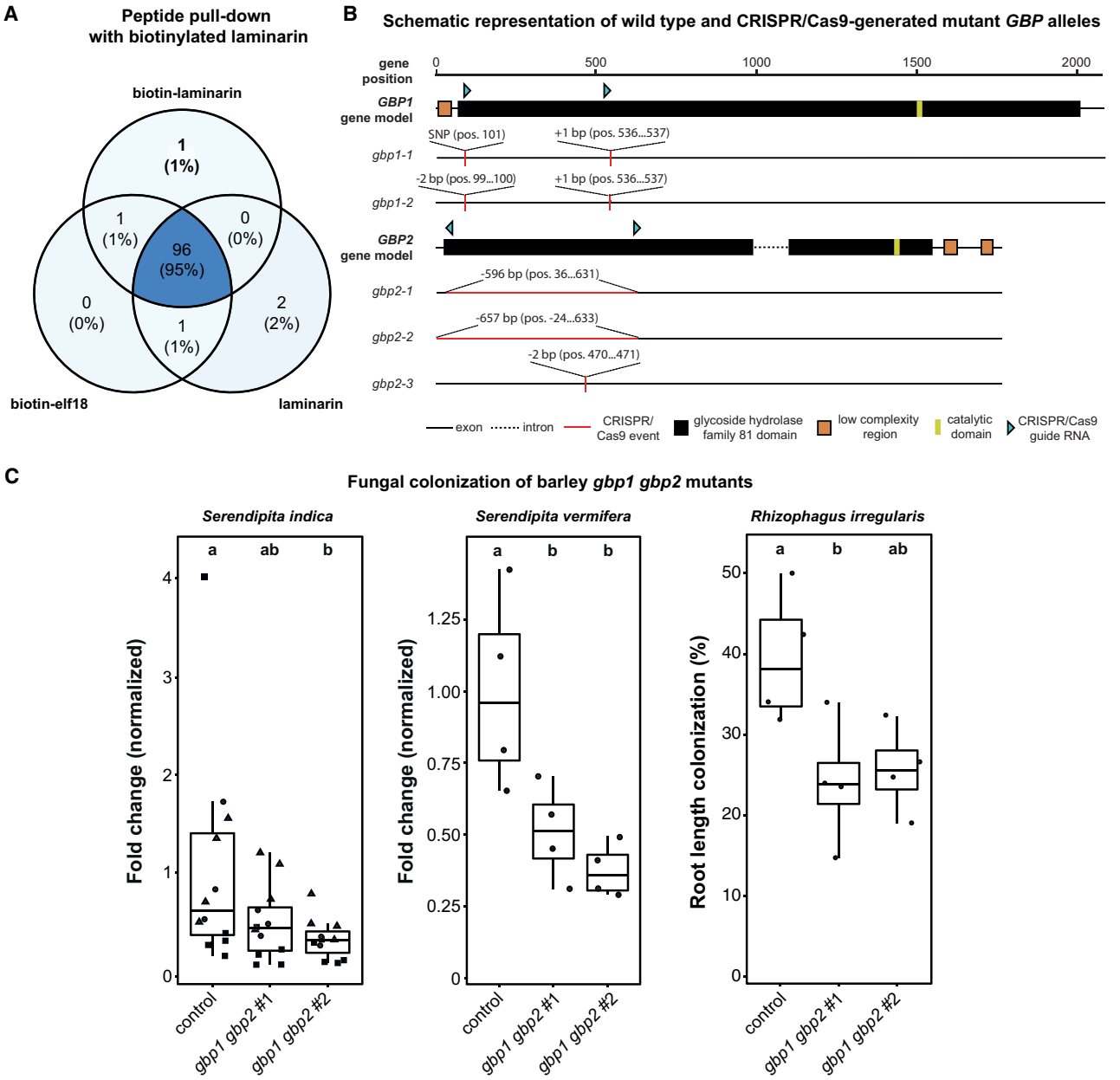

Figure 1. GBP1 is a compatibility factor identified via protein pull-down with biotinylated β-glucan in barley

(A) Venn diagram of barley proteins identified by liquid chromatography-tandem mass spectrometry (LC-MS/MS) analysis with biotinylated β-glucan laminarin, biotinylated elf18 (peptide derived from bacterial elongation factor Tu), or non-biotinylated β-glucan laminarin as bait. Only the proteins whose peptides were identified in three out of four replicates are listed.

(B) Schematic overview of CRISPR-Cas9-generated mutant alleles of *GBP1* and *GBP2*.

(C) Fungal colonization assays in roots of control and *gbp1 gbp2* mutant lines. The expression of *S. indica* and *S. vermifera* housekeeping genes was quantified by RT-PCR and normalized to the barley housekeeping gene ubiquitin (*HvUBI*). *R. irregularis* colonization was assessed using light microscopy to quantify the presence of ink-stained *R. irregularis* structures in roots. Root sections were considered to be colonized when arbuscules, intraradical hyphae (IRH), or vesicles were present. A total of 300 randomly chosen sections (covering 30 cm of root) were analyzed per replicate (n = 4).

Boxplot elements in this figure: center line, median; box limits, upper and lower quartiles; whiskers, 1.5× interquartile range. Data points from independent experiments are indicated by different shapes. Different letters represent statistically significant differences based on one-way ANOVA and Tukey's post hoc test (significance threshold: $p \leq 0.05$).

See also Figures S1–S3 and Tables S1, S2, and S3.

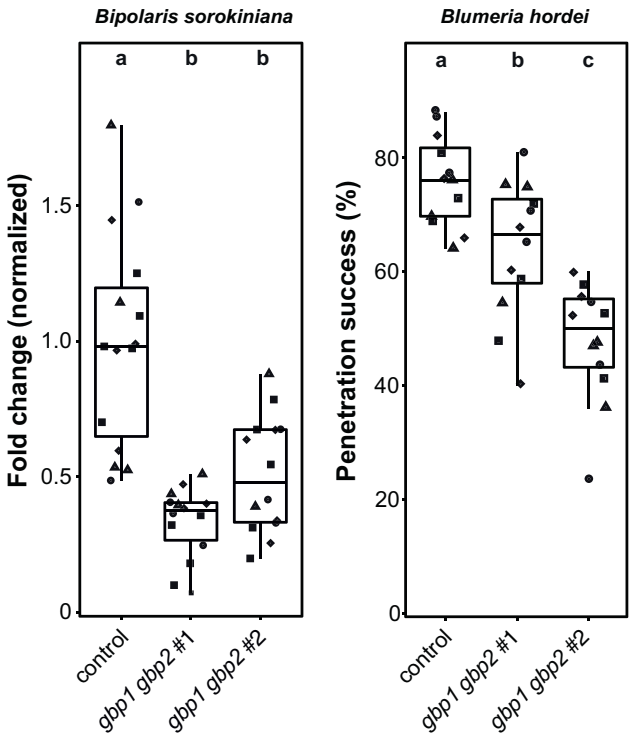

Figure 2. Mutation of barley *GBP1 GBP2* decreases colonization by the fungal pathogens *B. sorokiniana* and *B. hordei*

To test the impact of *GBP* mutation on the compatibility of pathogenic fungi, barley roots and shoots were inoculated with *B. sorokiniana* (left graph) and *B. hordei* (right graph), respectively. Barley control and *gbp* mutant lines were inoculated with *B. sorokiniana* and grown in jars under axenic conditions for 7 days (Figure S3C). To assess the degree of root colonization, the expression of *B. sorokiniana* housekeeping gene *BsTEF* was quantified by RT-PCR and normalized to the barley housekeeping gene ubiquitin *HvUBI*. Barley leaves colonized by *B. hordei* were analyzed for penetration success using bright-field microscopy (Figure S3D). Boxplot represents quantification of *B. hordei* penetration success at 48 h. Boxplot elements in this figure: center line, median; box limits, upper and lower quartiles; whiskers, 1.5× interquartile range. Data points from independent experiments are indicated by data point shape. Different letters represent statistically significant differences based on one-way ANOVA and Tukey's post hoc test (significance threshold: $p \leq 0.05$). See also Figure S3 and Tables S2 and S3.

two *GBP* copies (*GBP1* and *GBP2*, HORVU6Hr1G034610.3), but only *GBP1* is expressed according to publicly available transcriptomic datasets and our own expression analyses.[41]

To investigate the contribution of barley GBPs to fungal colonization, we used a CRISPR-Cas9 approach to generate plants mutated in both *GBP* genes (*gbp1 gbp2*; Figure 1B). We used spring barley (*H. vulgare* L.) cv. Golden Promise Fast[42] (hereafter, control line) as genetic background for the mutations. The first mutant line (*gbp1 gbp2* #1) is homozygous for the mutant alleles *gbp1-1* and *gbp2-1*, and the second mutant line (*gbp1 gbp2* #2) is homozygous for the *gbp1-2 allele* and biallelic for *gbp2-2* and *gbp2-3*. The seedlings of the two independent mutant lines showed no obvious differences in root and shoot biomass or length compared with the non-mutagenized control line (Figure S2). To survey colonization by fungi with different lifestyles and colonization strategies, we inoculated the control and both mutant lines with the beneficial root endophytes *S. indica* and *S. vermifera* as well as the AM fungus *R. irregularis* (Figures 1C, S3A, and S3B). In all three cases, total fungal colonization was reduced in both *gbp1 gbp2* mutant lines compared with the control line, with at least one mutant line presenting a significant reduction in colonization. To expand the range of surveyed fungal lifestyles, we additionally tested colonization by the hemibiotrophic root pathogen *B. sorokiniana* (Figures 2 and S3C) and the obligate biotrophic foliar pathogen *B. hordei* (Figures 2 and S3D). *B. sorokiniana* showed a significant decrease of fungal biomass, and *B. hordei* penetration success was inhibited at 48 h post infection (Figure 2). In conclusion, the *gbp1 gbp2* mutant lines showed increased resistance to fungal colonization compared with the control plants, irrespective of the taxonomic position of the fungus, its lifestyle, or the host tissue inoculated. Although we cannot rule out the possibility that GBP2 is also involved in mediating compatibility, the fact that only nominal expression of *GBP2* was detected suggests that the observed phenotype mainly depends on the role of GBP1 as a compatibility factor for fungal colonization of root and leaf tissues.

GBP1 is an active β-1,3-endoglucanase hydrolyzing β-1,3-glucans with a low degree of β-1,6 substitutions

We further biochemically characterized the β-glucan-interactor GBP1, which belongs to the GH81 family of the CAZymes. Enzymes of this GH-family are characterized by their endoglycosidic hydrolase activity on substituted and unsubstituted β-1,3-linked glucans. Their catalytic center is highly conserved across bacteria, fungi, and plants. GH81 family glycosyl hydrolases follow an inverting hydrolysis mechanism that requires a glutamate residue acting as nucleophile (Figure 3A).

To verify the predicted β-1,3-endoglycosidase activity of GBP1, we overexpressed and purified a codon-optimized, C-terminally HA-StrepII-tagged version of barley GBP1 from transiently transformed *N. benthamiana* leaves. Digestion assays with laminarin as a substrate confirmed the β-1,3-endoglycosidase activity of GBP1 (Figure 3B). Furthermore, site-directed mutagenesis of the predicted catalytically active site of GBP1 by replacing the first glutamate residue (putative nucleophile, E500) with an alanine ($GBP1_{E500A}$) abolished its enzymatic activity (Figure 3B). This confirms that the observed digestion of laminarin is dependent on the conserved catalytic site of GBP1. GBP1 activity is specific to the tested β-1,3-linked glucans (laminarihexaose, laminaritriose, and laminarin), whereas MALDI-TOF analysis revealed that GBP1 is unable to digest other oligosaccharides such as β-1,4-linked cellohexaose and xyloglucan (XXXG) (Figures 3B and 3C). Digestion of laminarin gradually leads to an accumulation of laminaribiose, with a minor fraction of glucose being released (Figures 4A and 4B). Activity assays with laminarin showed that GBP1 is highly active over a wide range of pH values (pH 5–9) and has the highest hydrolytic activity at 60°C (Figures 4C, S4A, and S4B).

To further test whether GBP1 is able to process complex substrates derived from the CW and EPS matrix of fungi, we performed digestion assays with crude *S. indica* CW and EPS matrix preparations as well as the previously characterized β-GD.[33] β-GD is a glucan fragment that is highly enriched during

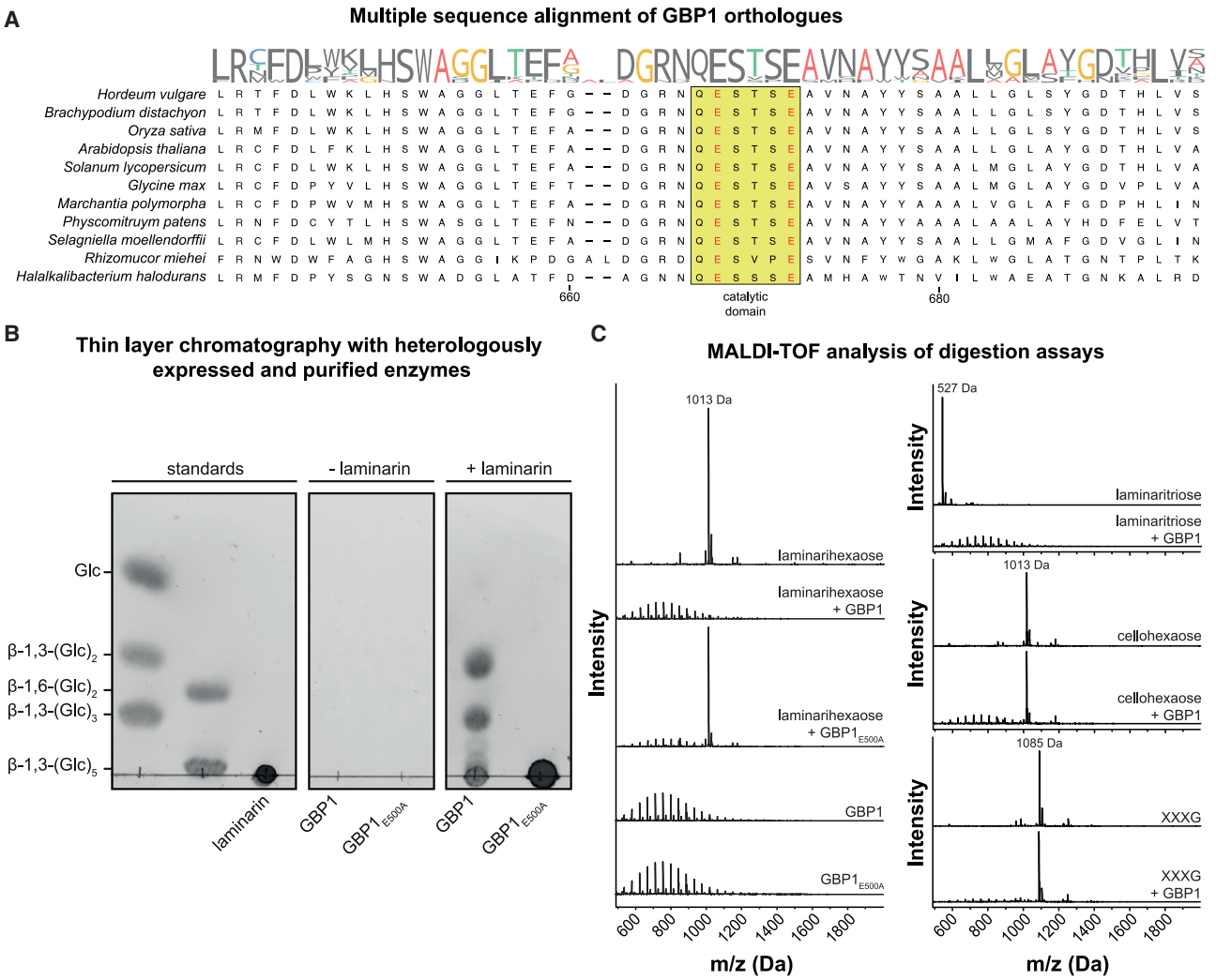

Figure 3. Barley GBP1 has a conserved GH81 catalytic center that specifically mediates the hydrolysis of β-1,3-glucans

(A) Multiple sequence alignment with sequences from different domains of life indicates conservation of nucleophilic glutamate residues (red letters) within the catalytic domain (yellow box).

(B) Analysis of the β-1,3-glycosidic activity of heterologously expressed and purified GBP1 and mutant GBP1$_{E500A}$ on laminarin from *Laminaria digitata*. After overnight incubation at 25°C, the digestion products were analyzed by thin-layer chromatography. The experiment was repeated at least four times with similar results.

(C) The activity of GBP1 and GBP1$_{E500A}$ was tested on laminarihexaose (β-1,3-glucan hexamer), laminaritriose (β-1,3-glucan trimer), cellohexaose (β-1,4-glucan hexamer), and XXXG (xyloglucan heptasaccharide). After overnight digestion at 25°C, the products were analyzed by MALDI-TOF mass spectrometry. The ion signal ladder between 500 and 1,000 Da represents an unknown contamination present in the GBP1 preparation and is thus unrelated to any digested carbohydrate. Digestion assays were performed twice with similar results. UT, untreated; XXXG, xyloglucan heptasaccharide.

See also Figure S4.

digestion of the *S. indica* matrix by the barley glucanase BGLUII. Although GBP1 does not hydrolyze the highly β-1,6-branched glucans in the EPS matrix of *S. indica* and the derived β-GD, it releases oligosaccharides (DP 7–13) from *S. indica* CWs to a limited extent (Figure S4C). This is consistent with the inability of GBP1 to digest the highly substituted laminarin from the brown alga *Eisenia bicyclis* (Figure S5A). These results verify the protective role of frequent β-1,6-branching patterns of glucans against hydrolytic degradation and activation of plant immunity as previously demonstrated for the EPS matrices of plant-colonizing fungi.[33]

Secreted plant hydrolases are known to modulate the activation of immunity by releasing, tailoring, and increasing the accessibility of fragments from invading microbes.[28,43] To investigate to what extent the observed hydrolytic activity of GBP1 on β-1,3-glucans alters their immunogenic potential, we treated *N. benthamiana* and barley with gradually digested laminarin (Figure 5). We used β-glucan-triggered ROS production, one of the first signaling outputs triggered by MAMPs,[44] as a readout to assess changes in early immune signaling. *N. benthamiana* and barley differ in terms of their perceived β-glucan substrates.[31] The dicotyledonous *N. benthamiana*

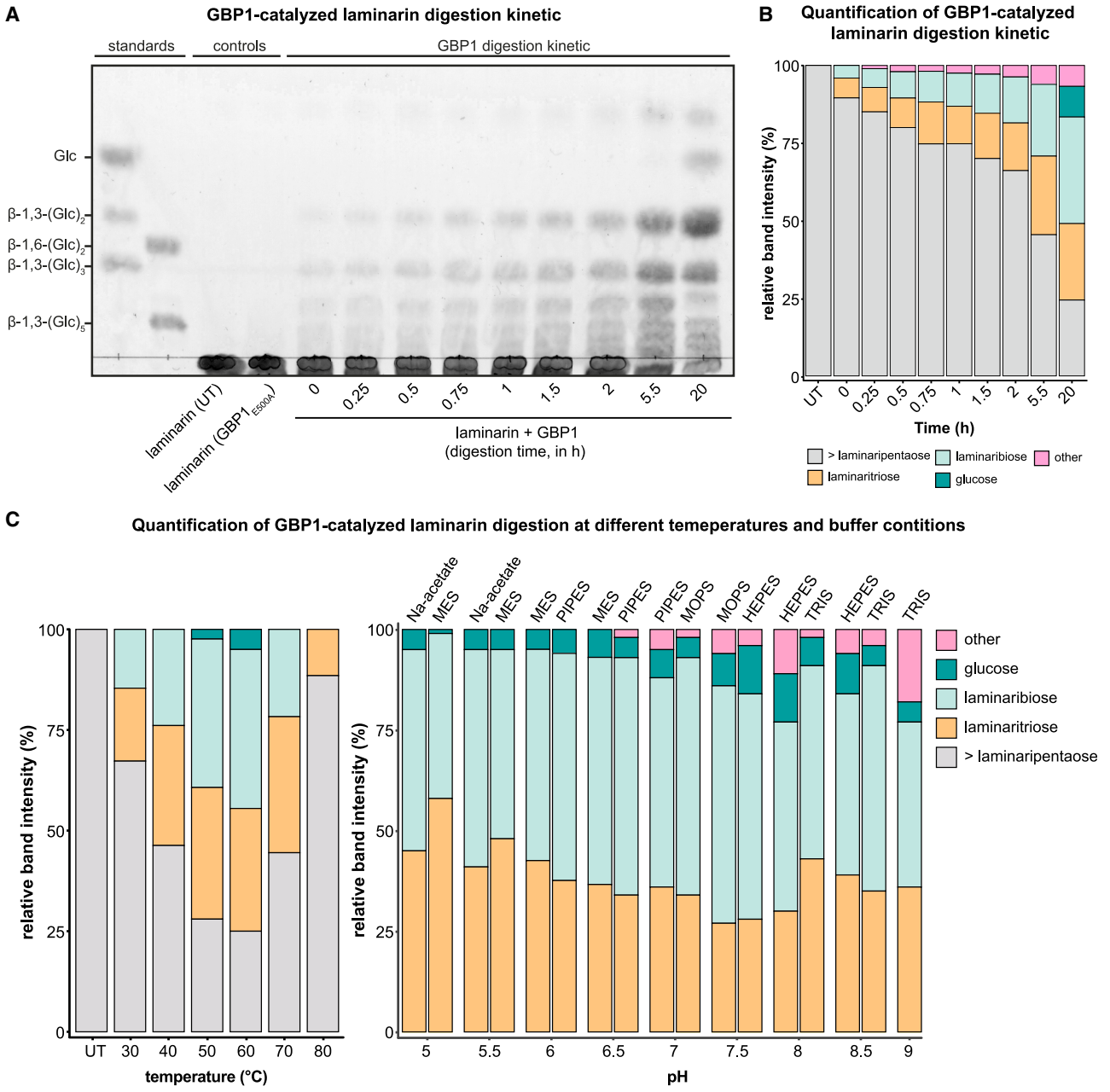

Figure 4. Biochemical characterization of GBP1 activity on laminarin

(A) The digestion products resulting from the enzymatic breakdown of laminarin by GBP1 over time were analyzed using thin-layer chromatography (TLC). Untreated (UT) and $GBP1_{E500A}$-treated laminarin (20 h) served as controls. Digestion was performed at 25°C.

(B) Quantification of GBP1-catalyzed laminarin digestion products. TLC band intensity was quantified using the ImageJ software.

(C) Laminarin (4 mg·mL^{-1}) was digested with GBP1 (70 nM) for 10 min at different temperatures (left graph) or in different buffers (10 mM, pH 5–9, right graph). Products from GBP1-catalyzed laminarin digestion assays were separated by TLC (Figures S4A and S4B) and quantified via ImageJ. UT, untreated.

See also Figures S4 and S5.

activates immune responses when treated with long-chain β-1,3-glucans. As digestion of laminarin by GBP1 progressed, the intensity of the triggered oxidative burst gradually decreased to the level of mock treatment (20 h) (Figure 5A). In contrast to *N. benthamiana*, barley responds to both short- and long-chain β-1,3-glucans. Accordingly, incubation of laminarin with GBP1 reduced the intensity of the oxidative burst but did not completely abolish it due to the recognition of the released short-chain hydrolysis products (Figure 5B). Treatment with the inactive version $GBP1_{E500A}$ (20 h) did not affect laminarin perception in either species (Figures 5A and 5B).

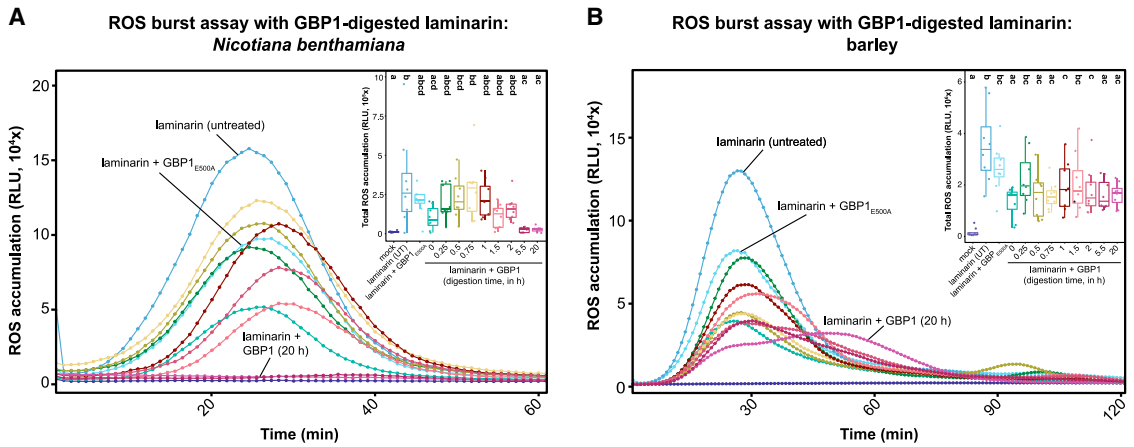

Figure 5. GBP1 treatment of long-chain β-1,3-linked glucans modulates ROS production

Apoplastic ROS accumulation after treatment of *N. benthamiana* (A) and barley (B) with gradually digested laminarin (1 mg·mL^{-1}) was monitored using a luminol-based chemiluminescence assay. Milli-Q water (mock) treatment, untreated laminarin (UT), and $GBP1_{E500A}$ were used as controls. Values represent mean from eight replicates. Boxplots display total ROS accumulation over the measured period of time. The assays were performed two times with independent laminarin digestions. Boxplot elements in this figure: center line, median; box limits, upper and lower quartiles; whiskers, 1.5× interquartile range. Different letters represent statistically significant differences in relative luminescence units (RLU) based on a one-way ANOVA and Tukey's post hoc test (significance threshold: $p \leq 0.05$). ROS, reactive oxygen species; RLU, relative luminescence units.

See also Table S3.

Barley GBPs are not essential for β-glucan-triggered ROS production

Previous studies on perception of a β-1,3/1,6-heptaglucoside from oomycetes in legumes suggested that GBPs may be part of the corresponding β-glucan perception machinery.[40,45] Since oomycete-derived heptaglucoside perception is specific to legumes,[45] we investigated whether barley GBPs are involved in β-glucan-triggered ROS production upon treatment with short- and long-chain β-glucans. Since ROS production still occurred in both *gbp* double-mutant lines (Figure S5C), we conclude that GBPs are not essential for the immune perception of β-glucan in barley.

Barley *gbp* mutants exhibit a hyper-responsive CW reaction upon colonization by endophytic fungi

Previous studies have shown that broad-spectrum resistance to fungi can be mediated by the enhanced formation of CWAs, so-called papillae, which are predominantly formed at the sites of hyphal penetration.[46] A major component of these CW reinforcements is callose, a linear β-1,3-linked glucan that could serve as a substrate for GBPs. To investigate the effect of GBPs on the formation of CWAs upon colonization by the root endophyte *S. indica*, we monitored and quantified CWAs using a fluorescent version of the carbohydrate-binding lectin concanavalin A (Con A), which has been shown to accumulate at the CWAs in barley in previous studies.[46,47] Papilla formation was observed in all barley lines tested after colonization with the fungus, with no differences in papilla size or frequency between the control line and the two *gbp1 gbp2* mutant lines (Figure S6A). However, in addition to round-shaped papillae, inoculated mutant roots exhibited an extensive response lining the CWs of the epidermal root cells (Figures 6A–6C). These excessive, atypical responses at the host CW (hereafter, CW hyper-responses) occurred exclusively when colonized by the fungus and not in plants grown without the fungus under control conditions (Figure S6B). Staining of *S. indica*-colonized barley roots with aniline blue, a commonly used stain to detect callose CW depositions, revealed elongated regions of deposited callose in the *gbp* double mutants (Figure S6C), which resembled the CW hyper-responses previously observed with Con A staining (Figure 6A). By contrast, the control line exhibited only small round callose depositions during *S. indica* colonization (Figure S6C). To test whether the observed CW hyper-responses are accompanied by enhanced activation of other defense responses, we quantified transcript levels of *PATHOGENESIS-RELATED PROTEIN 10* (*PR10*), a commonly used defense marker gene in barley. Mock-treated *gbp1 gbp2* mutants exhibited an increased *PR10* basal expression (Figure 6D). Upon *S. indica* colonization, *PR10* expression was more strongly induced in both *gbp1 gbp2* mutant lines compared with the control line (Figure 6D). This indicates that *gbp* double mutants present stronger induction of defense responses during fungal colonization.

DISCUSSION

The success of fungal colonization is largely determined by the environmental conditions (e.g., nutrient availability) and genetic factors of the host. Depending on the type of plant-fungal interaction, these genetic factors are referred to as susceptibility factors (pathogenic interaction) or compatibility factors (beneficial interaction). Their mutation can interfere with fungal colonization at different stages by hampering tissue penetration and early establishment, by modulating the plant immune system, or by removal of structural and metabolic components that are required for fungal maintenance.[48] In AM symbiosis, compatibility is additionally mediated by a set of evolutionary conserved genes that are exclusively present in AM host species.[49,50] In cooperation with membrane-integral LysM receptor kinases, these components

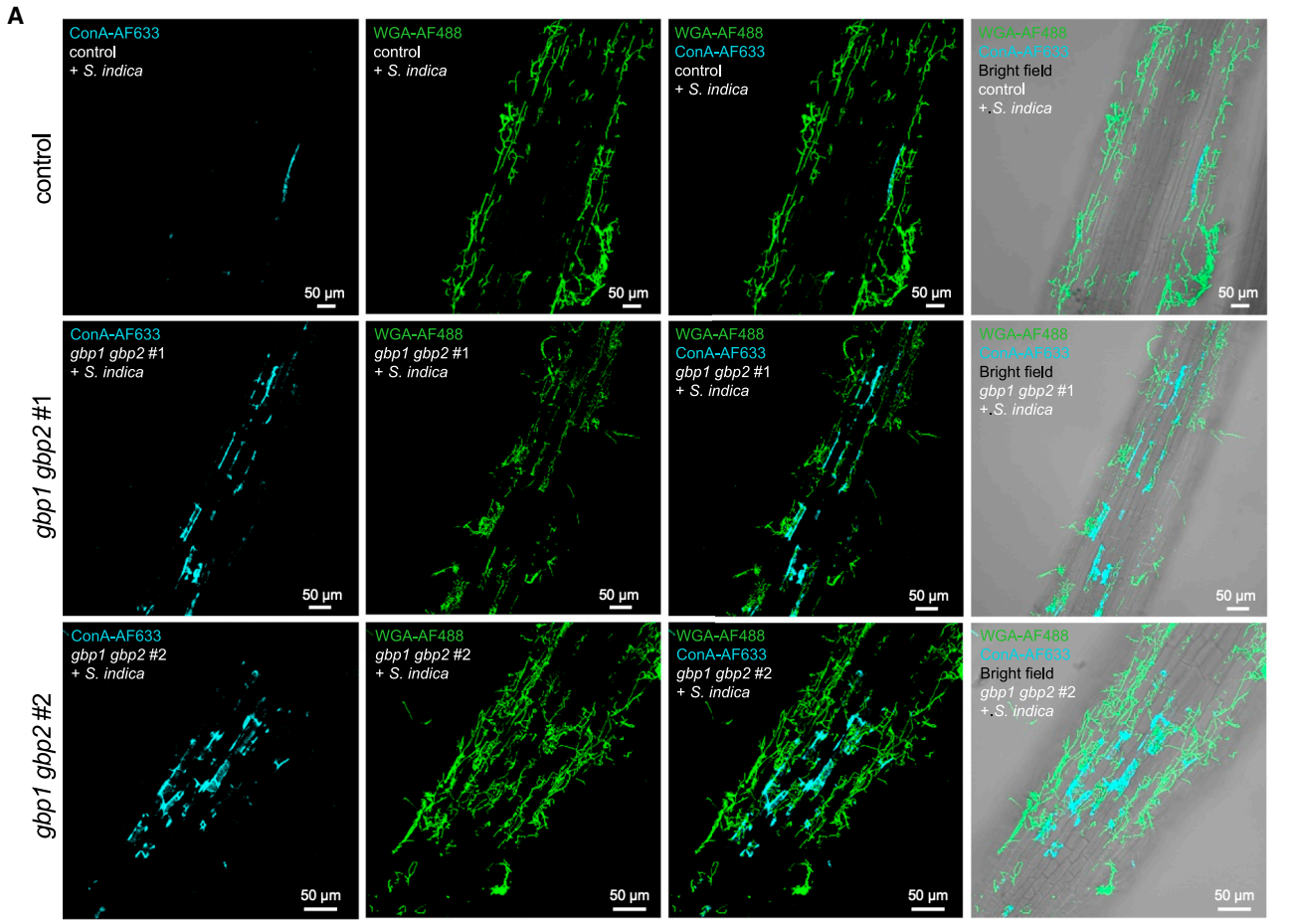

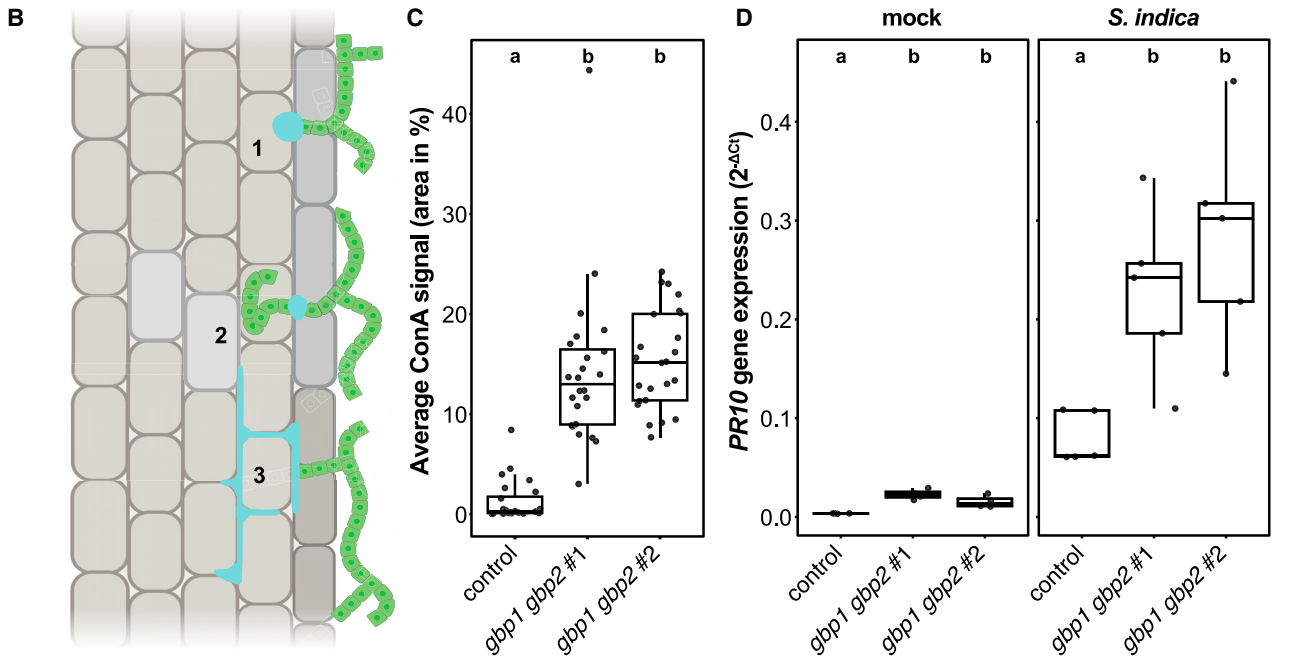

(legend on next page)

are responsible for the signal transduction and decoding of nuclear calcium spiking signatures triggered by microbial chitin-derived oligomers. Although this pathway is considered to be specific for the accommodation of AM fungi, many endophytes and pathogens can exploit it, at least partially, to ensure their own establishment within the host.[51–55] Many fungi have adapted their colonization strategies to fundamental developmental processes, for example, by relying on the host's CW structure and membrane dynamics for successful establishment within host tissue. Interferences of these processes can massively impact fungal compatibility.[48]

In this study, we present a previously undescribed role of GBPs, a family of GH81-type β-1,3-endoglucanases, as tissue-independent, broad-spectrum compatibility factors that enhance fungal colonization. Barley GBP1 was identified as a β-glucan interactor by a pull-down approach using laminarin as a β-1,3-glucan bait (Figure 1A). Laminarin is an algal storage carbohydrate that commonly serves as a commercially available surrogate for fungal cell surface glycans due to its β-1,3/1,6-linkage pattern.[27,30] Plant β-1,3-glucanases are involved in plant development and plant-microbe interactions.[29] In the context of plant immunity, β-1,3-endoglucanases became known as PR group 2 (PR2) proteins due to their expression pattern upon plant defense activation. Contrasting with the primary role of β-1,3-endoglucanases in plant resistance, we show that knocking out the only two GBP paralogs in barley leads to reduced colonization by the mutualistic root endophytes *S. indica* and *S. vermifera*, as well as the AM fungus *R. irregularis* (Figure 1). This suggests that barley GBPs serve as compatibility factors for colonization by beneficial root fungi. This compatibility principle was found to extend beyond mutualistic fungi, as colonization by the hemibiotrophic root pathogen *B. sorokiniana* as well as the biotrophic foliar pathogen *B. hordei* was similarly hindered (Figure 2). Fluorescence microscopy revealed that reduced colonization by the mutualistic fungus *S. indica* in the *gbp1 gbp2* mutants was accompanied by a strong response at the host CW, as stained with the lectin Con A (Figure 6). These callose-containing CWAs were not spatially restricted to the sites of fungal penetration but instead excessively and amorphously spread along the host CW within the colonized area (Figures 6 and S6). In addition to the observed changes in CW callose deposition, *gbp1 gbp2* double mutants had increased baseline expression levels of the defense-related marker gene *PR10* and exhibited a significantly higher induction of *PR10* expression upon treatment with *S. indica* (Figure 6D). Since we did not observe spontaneous CWA formation nor excessive activation of *PR10* expression in mock-treated plants, constitutive activation of defense responses by *GBP* mutation is unlikely (Figures 6D and S6B).

The contribution of papillae formation to fungal resistance has been controversial over the last decades; however, several studies reported that both early and increased papillae formation can protect hosts from fungal penetration.[7,9] Arabidopsis plants constitutively over-expressing the callose synthase *PMR4* produced enlarged callose depositions at the inner and outer side of the cellulosic CW at early time points of fungal infection.[56,57] This mediates complete penetration resistance to adapted and non-adapted powdery mildew strains without the induction of either SA- or JA-dependent pathways.[56] Callose depositions induced by defense priming also enhanced resistance to the necrotrophic pathogens *Alternaria brassicicola* and *Plectosphaerella cucumerina* in Arabidopsis.[58] Moreover, *mildew resistance locus O* (*mlo*)-dependent resistance of barley to *B. hordei* and *S. indica* is accompanied by a faster formation of larger papillae in leaves or roots, respectively.[8,46,59,60] Similar to our observations for the *gbp1 gbp2* mutants, barley *mlo* mutants also exhibited impaired colonization by AM fungi during early stages of interaction.[61] This decrease in colonization by mutualistic fungi may partially explain why genes contributing to pathogen infection have been conserved throughout evolution. Mutations of compatibility genes often bring along developmental penalties (e.g., growth, yield) or increased susceptibility to pathogens with other infection strategies.[48] However, we did not observe any differences in root and shoot fresh weight or root and shoot length between the control line and the *gbp1 gbp2* mutants (Figure S2). Although barley *mlo* mutants were more susceptible to necrotrophic and hemibiotrophic foliar pathogens due to the spontaneous occurrence of cell death,[62,63] barley *gbp1 gbp2* mutants exhibited reduced colonization by the aggressive hemibiotrophic root pathogen *B. sorokiniana*. Future studies should survey the colonization rates of further root (e.g., *Fusarium graminearum*, *Rhizoctonia solani*) and leaf (e.g., *Pyrenophora teres* f. sp. *teres*, *Rhynchosporium secalis*) necrotrophs.

The causal link between the *gbp1 gbp2* mutations and increased defense responses that lead to reduced fungal compatibility remains yet to be clarified. Barley GBP1 could process β-glucan-based host or MAMPs released during fungal colonization to modulate immune response activation as fungal colonization progresses. Missing GBP activity could lead to an overaccumulation of long-chain β-glucan elicitors in the host

Figure 6. Colonization of barley *gbp1 gbp2* mutant lines by *S. indica* results in CW hyper-response and enhanced *PR10* expression

(A) Barley root CW responses of control and *gbp1 gbp2* mutant lines colonized by *S. indica*. Samples were fluorescently labeled with concanavalin A (Con A-AF633, cyan) and wheat germ agglutinin (WGA-AF488, green) for visualization of CWAs and fungal structures, respectively, then analyzed by confocal laser scanning microscopy.

(B) Schematic representation of different forms of CWAs in barley roots in response to fungal colonization. These include papillae formation at the sites of attempted (1) and successful (2) hyphal penetration, as well as an extensive reaction along the CWs (3).

(C) Percent area of the root showing CW response in barley control and *gbp1 gbp2* mutant lines. Letters represent statistically significant differences in Con A signal based on a Kruskal-Wallis test and Dunn's post hoc test (significance threshold: $p \leq 0.05$, $n = 24$).

(D) Barley control and *gbp1 gbp2* mutant lines were inoculated with sterile water (mock) or *S. indica* and grown under axenic conditions. Root tissues were harvested at 6 days post inoculation (dpi). The expression of the barley defense gene *HvPR10* was analyzed by RT-PCR and normalized to the barley housekeeping gene *HvUBI*.

Data were analyzed by one-way ANOVA and Tukey's post hoc test (significance threshold: $p \leq 0.05$). Con A, concanavalin A; CW(A), cell wall (appositions); WGA, wheat germ agglutinin.

See also Figure S6 and Tables S2 and S3.

apoplast, possibly explaining the large-scale induction of CW responses observed in the *gbp1 gbp2* mutant background upon *S. indica* colonization. A related homeostasis principle was recently demonstrated for berberine bridge enzyme-like oxidases that counteract the deleterious accumulation of active oligogalacturonides and cellodextrins as DAMPs in the host apoplast during microbial colonization.[64,65] GBPs could also be involved in the release or tailoring of a yet undescribed β-glucan-derived signaling molecule that dampens immunity to facilitate colonization of mutualistic fungi.[66,67] Similar to β-glucans, symbiotic signals such as short chitooligosaccharides (e.g., chitotetraose) and lipo-chitooligosaccharides are abundantly found in both symbiotic and pathogenic fungi and fulfill various functions relevant for inter-kingdom interactions.[68,69] Only recently, an EPR3-type receptor kinase in *Lotus japonicus* was shown to promote intracellular accommodation of fungi through binding to well-defined β-1,3/β-1,6 glucan fragments derived from the EPS matrix of *S. indica* and *B. sorokiniana*.[67] Alternatively, GBP1 could be an important factor for dynamic adjustment of CW responses. The β-1,3-glucan callose is—along with phenolic substances and other CW carbohydrates—a major component of CWAs.[8,9] GBPs could directly degrade the callose in defense-triggered CWAs, thus acting as a negative regulator of CWA formation. In support of this hypothesis, enlarged depositions of callose were observed in the *gbp1 gbp2* mutant lines upon *S. indica* colonization (Figure S6C).

In the apoplastic space, the hydrolytic activity of β-1,3-endoglucanases contributes to host immunity in multiple ways.[29] Secreted β-1,3-glucanases directly process the β-glucan-containing surface glycans of invading fungi and oomycetes. Furthermore, this hydrolytic activity leads to the release of glucan fragments that can act as elicitors of plant defense responses. Since the outermost layer of fungal cell surface glycans mainly consists of β-1,3-glucans,[27] hydrolysis by β-1,3-glucanases renders the inner chitin layer more accessible to secreted plant chitinases. Although GH81 family members are not categorized as PR2 proteins, previous studies focusing on GBPs from soybean, and other legumes have shown their importance in defense against oomycetes.[45,70] To better understand the contribution of GBP1 to hydrolysis of fungal surface glycan substrates, we performed substrate characterization assays with heterologously purified barley GBP1. GBP1 specifically hydrolyzes linear β-1,3-glucans as short as laminaritriose (Figure 3C) but did not effectively act on preparations of the EPS matrix or CW isolated from *S. indica* (Figure S4C). EPS matrices from a variety of plant-colonizing fungi consist of a β-1,3-linked glucan backbone heavily substituted with β-1,6-linked glucose.[26,33] Barley BGLUII, an enzyme secreted upon confrontation with fungi, has been shown to release a β-glucan decasaccharide with antioxidative properties from this EPS matrix that facilitates fungal colonization.[33] Since GBP1 was unable to digest highly substituted laminarin from *E. bicyclis*,[71,72] we conclude that the high degree of branching in the EPS matrix similarly protects this cell surface glycan from hydrolysis by GBP1 (Figures S5A and S5B). However, we cannot exclude that cell surface glycans from other fungi or oomycetes might serve as better substrates for GBP1. Although GBP1 from barley did not exhibit a pioneering hydrolytic role on the tested preparations, in a more complex scenario with a variety of secreted host hydrolases, GBP1 could belong to a second set of hydrolytic enzymes acting on the predigested cell surface glycans of microbial invaders. In the performed ROS burst assays, we observed that treatment of the long β-glucan laminarin with GBP1 differentially modulated ROS production in the two tested species (Figure 5), demonstrating that GBP1 has the potential to fine-tune ROS homeostasis.

Soybean GBPs contain two carbohydrate-associated domains: an endoglycosidic hydrolase domain and a high-affinity binding site for a *Phytophthora sojae*-derived β-glucan heptaglucoside elicitor.[45] Inhibition of elicitor binding to GBP with a specific antibody prevented the production of phytoalexins, suggesting that soybean GBP may be part of the β-glucan-heptaglucoside receptor complex.[40] Since GBP1 was identified by a pull-down using laminarin, we hypothesize that GBP1 has a β-glucan-binding domain in addition to the hydrolytic domain. However, ROS production in barley *gbp1 gbp2* lines is not reduced upon treatment with various β-glucan elicitors, ruling out the long-standing hypothesis that barley GBPs are necessary components of a β-1,3-glucan receptor complex involved in immunity.[45] Functional differences between barley and legume GBPs are not surprising given the massive expansion of GBPs in the legume family, suggesting that legume GBPs may have diversified in terms of their role upon a multitude of various abiotic and biotic stresses and accommodation of beneficial microbes as suggested for the *MLO* family members.[61] Consistent with the enhancing role of barley BGLUII in fungal colonization, our findings provide new insights of how spatiotemporal dynamics in perception and hydrolysis of host and microbial β-glucans modulate fungal establishment in the host tissue.

For decades, plant β-1,3-glucanases were predominantly considered to be deployed as a defensive strategy to hinder microbial invasion. Our work shows that β-1,3-glucanases such as barley GBPs can play a previously undescribed role as compatibility factors for colonization by fungi of different phylogenetic origins and lifestyles. Our findings provide new insights into the contribution of host β-glucanases to spatiotemporal dynamics in perception and degradation of host and microbial β-glucans that promote fungal establishment in the host tissue.

STAR★METHODS

Detailed methods are provided in the online version of this paper and include the following:

- KEY RESOURCES TABLE
- RESOURCE AVAILABILITY
  - Lead Contact
  - Materials Availability
  - Data and Code Availability
- EXPERIMENTAL MODEL AND SUBJECT DETAILS
  - Plant material and growth conditions
  - Fungal material, growth conditions and barley colonization assays
- METHOD DETAILS
  - Carbohydrate substrates for immunity and enzymatic digestion assays

- Identification of protein candidates interacting with β-glucan
- Plasmid construction for the heterologous expression of barley GBP1 in *N. benthamiana*
- Heterologous protein production and purification from *N. benthamiana*
- Oxidative burst assay
- MALDI-TOF analysis
- CRISPR/Cas9-based mutagenesis of GBP homologues in barley
- Staining for confocal microscopy

- QUANTIFICATION AND STATISTICAL ANALYSES

SUPPLEMENTAL INFORMATION

Supplemental information can be found online at https://doi.org/10.1016/j.cub.2023.10.048.

ACKNOWLEDGMENTS

We thank Hanna Rovenich, Dennis Mahr, Daniela Niedeggen, and Edelgard Wendeler for technical support. We thank Gregor Langen for the bioinformatic support and the discussions. A.Z., M.P., P.S., I.M.L.S., and B.C. acknowledge support from the Cluster of Excellence on Plant Sciences (CEPLAS) funded by the Deutsche Forschungsgemeinschaft (DFG, German Research Foundation) under Germany's Excellence Strategy–EXC 2048/1–Project ID: 390686111. A.Z. and L.K.M. acknowledge support from project ZU 263/11-1 (SPP 2125 DECRyPT). A.W., S.v.B., and L.K.M. acknowledge support by the International Max Planck Research School (IMPRS) on "Understanding Complex Plant Traits using Computational and Evolutionary Approaches" and the University of Cologne. I.M.L.S. was funded by the DFG Emmy Noether Programme (SA 4093/1-1). P.D., N.H., F.L.H.M., and C.Z. acknowledge support from the Gatsby Charitable Foundation.

AUTHOR CONTRIBUTIONS

A.W., S.W., and A.Z. conceived the study. S.W., N.H., P.D., F.L.H.M., and C.Z. directed and supervised the protein pull-down. I.F.A. and A.W. generated the barley CRISPR-Cas9 mutants. L.K.M., S.v.B., M.B., and I.M.L.S. performed the fungal colonization assays. A.W., M.N., and P.S. performed the biochemical experiments. B.C., A.Z., and M.P. directed and supervised the carbohydrate analytics. A.W. and A.Z. supervised the project and designed the experiments. A.W., S.v.B., and A.Z. wrote the paper with the contributions from all the authors.

DECLARATION OF INTERESTS

The authors declare no competing interests.

Received: April 1, 2023
Revised: August 6, 2023
Accepted: October 25, 2023
Published: November 16, 2023

REFERENCES

1. Cosgrove, D.J. (2005). Growth of the plant cell wall. Nat. Rev. Mol. Cell Biol. *6*, 850–861.
2. Cosgrove, D.J., and Jarvis, M.C. (2012). Comparative structure and biomechanics of plant primary and secondary cell walls. Front. Plant Sci. *3*, 204.
3. Aist, J.R. (1977). Papilla formation: timing and significance during penetration of barley coleoptiles by Erysiphe graminis hordei. Phytopathology *77*, 455. https://doi.org/10.1094/Phyto-67-455.
4. Brown, I., Trethowan, J., Kerry, M., Mansfield, J., and Bolwell, G.P. (1998). Localization of components of the oxidative cross-linking of glycoproteins and of callose synthesis in papillae formed during the interaction between non-pathogenic strains of Xanthomonas campestris and French bean mesophyll cells. Plant J. *15*, 333–343.
5. Bednarek, P., Pislewska-Bednarek, M., Svatos, A., Schneider, B., Doubsky, J., Mansurova, M., Humphry, M., Consonni, C., Panstruga, R., Sanchez-Vallet, A., et al. (2009). A glucosinolate metabolism pathway in living plant cells mediates broad-spectrum antifungal defense. Science *323*, 101–106.
6. Underwood, W. (2012). The plant cell wall: a dynamic barrier against pathogen invasion. Front. Plant Sci. *3*, 85. https://doi.org/10.3389/fpls.2012.00085.
7. Hückelhoven, R. (2007). Cell wall-associated mechanisms of disease resistance and susceptibility. Annu. Rev. Phytopathol. *45*, 101–127.
8. Chowdhury, J., Henderson, M., Schweizer, P., Burton, R.A., Fincher, G.B., and Little, A. (2014). Differential accumulation of callose, arabinoxylan and cellulose in nonpenetrated versus penetrated papillae on leaves of barley infected with Blumeria graminis f. sp. hordei. New Phytol. *204*, 650–660.
9. Hückelhoven, R. (2014). The effective papilla hypothesis. New Phytol. *204*, 438–440.
10. Molina, A., Miedes, E., Bacete, L., Rodríguez, T., Mélida, H., Denancé, N., Sánchez-Vallet, A., Rivière, M.-P., López, G., Freydier, A., et al. (2021). Arabidopsis cell wall composition determines disease resistance specificity and fitness. Proc. Natl. Acad. Sci. USA *118*, e2010243118, https://doi.org/10.1073/pnas.2010243118.
11. Gavrin, A., Rey, T., Torode, T.A., Toulotte, J., Chatterjee, A., Kaplan, J.L., Evangelisti, E., Takagi, H., Charoensawan, V., Rengel, D., et al. (2020). Developmental modulation of root cell wall architecture confers resistance to an oomycete pathogen. Curr. Biol. *30*, 4165–4176.e5.
12. Escudero, V., Jordá, L., Sopeña-Torres, S., Mélida, H., Miedes, E., Muñoz-Barrios, A., Swami, S., Alexander, D., McKee, L.S., Sánchez-Vallet, A., et al. (2017). Alteration of cell wall xylan acetylation triggers defense responses that counterbalance the immune deficiencies of plants impaired in the β-subunit of the heterotrimeric G-protein. Plant J. *92*, 386–399.
13. Hernández-Blanco, C., Feng, D.X., Hu, J., Sánchez-Vallet, A., Deslandes, L., Llorente, F., Berrocal-Lobo, M., Keller, H., Barlet, X., Sánchez-Rodríguez, C., et al. (2007). Impairment of cellulose synthases required for Arabidopsis secondary cell wall formation enhances disease resistance. Plant Cell *19*, 890–903.
14. Nishimura, M.T., Stein, M., Hou, B.-H., Vogel, J.P., Edwards, H., and Somerville, S.C. (2003). Loss of a callose synthase results in salicylic acid-dependent disease resistance. Science *301*, 969–972.
15. Yin, H., Du, Y., and Dong, Z. (2016). Chitin oligosaccharide and chitosan oligosaccharide: two similar but different plant elicitors. Front. Plant Sci. *7*, 522.
16. Albert, I., Hua, C., Nürnberger, T., Pruitt, R.N., and Zhang, L. (2020). Surface sensor systems in plant immunity. Plant Physiol. *182*, 1582–1596.
17. Hahn, M.G., Darvill, A.G., and Albersheim, P. (1981). Host-pathogen interactions: XIX. the endogenous elicitor, a fragment of a plant cell wall polysaccharide that elicits phytoalexin accumulation in soybeans. Plant Physiol. *68*, 1161–1169.
18. Liu, C., Yu, H., Voxeur, A., Rao, X., and Dixon, R.A. (2023). FERONIA and wall-associated kinases coordinate defense induced by lignin modification in plant cell walls. Sci. Adv. *9*, eadf7714.
19. Zarattini, M., Corso, M., Kadowaki, M.A., Monclaro, A., Magri, S., Milanese, I., Jolivet, S., de Godoy, M.O., Hermans, C., Fagard, M., and Cannella, D. (2021). LPMO-oxidized cellulose oligosaccharides evoke immunity in Arabidopsis conferring resistance towards necrotrophic fungus B. cinerea. Commun. Biol. *4*, 727.
20. Mélida, H., Bacete, L., Ruprecht, C., Rebaque, D., del Hierro, I., López, G., Brunner, F., Pfrengle, F., and Molina, A. (2020). Arabinoxylan-oligosaccharides act as damage associated molecular patterns in plants regulating disease resistance. Front. Plant Sci. *11*, 1210. https://doi.org/10.3389/fpls.2020.01210.

21. Zang, H., Xie, S., Zhu, B., Yang, X., Gu, C., Hu, B., Gao, T., Chen, Y., and Gao, X. (2019). Mannan oligosaccharides trigger multiple defence responses in rice and tobacco as a novel danger-associated molecular pattern. Mol. Plant Pathol. *20*, 1067–1079.

22. Claverie, J., Balacey, S., Lemaître-Guillier, C., Brulé, D., Chiltz, A., Granet, L., Noirot, E., Daire, X., Darblade, B., Héloir, M.-C., and Poinssot, B. (2018). The Cell wall-derived xyloglucan is a new DAMP triggering plant immunity in Vitis vinifera and Arabidopsis thaliana. Front. Plant Sci. *9*, 1725.

23. Ferrari, S., Savatin, D.V., Sicilia, F., Gramegna, G., Cervone, F., and Lorenzo, G.D. (2013). Oligogalacturonides: plant damage-associated molecular patterns and regulators of growth and development. Front. Plant Sci. *4*, 49.

24. Galletti, R., Denoux, C., Gambetta, S., Dewdney, J., Ausubel, F.M., De Lorenzo, G., and Ferrari, S. (2008). The AtrbohD-mediated oxidative burst elicited by oligogalacturonides in Arabidopsis is dispensable for the activation of defense responses effective against Botrytis cinerea. Plant Physiol. *148*, 1695–1706.

25. Aziz, A., Gauthier, A., Bézier, A., Poinssot, B., Joubert, J.-M., Pugin, A., Heyraud, A., and Baillieul, F. (2007). Elicitor and resistance-inducing activities of beta-1,4 cellodextrins in grapevine, comparison with beta-1,3 glucans and alpha-1,4 oligogalacturonides. J. Exp. Bot. *58*, 1463–1472.

26. Wawra, S., Fesel, P., Widmer, H., Neumann, U., Lahrmann, U., Becker, S., Hehemann, J.-H., Langen, G., and Zuccaro, A. (2019). FGB1 and WSC3 are in planta-induced β-glucan-binding fungal lectins with different functions. New Phytol. *222*, 1493–1506.

27. Wanke, A., Malisic, M., Wawra, S., and Zuccaro, A. (2021). Unraveling the sugar code: the role of microbial extracellular glycans in plant-microbe interactions. J. Exp. Bot. *72*, 15–35.

28. Rovenich, H., Zuccaro, A., and Thomma, B.P.H.J. (2016). Convergent evolution of filamentous microbes towards evasion of glycan-triggered immunity. New Phytol. *212*, 896–901.

29. Perrot, T., Pauly, M., and Ramírez, V. (2022). Emerging roles of β-glucanases in plant development and adaptative responses. Plants (Basel) *11*, 1119. https://doi.org/10.3390/plants11091119.

30. Fesel, P.H., and Zuccaro, A. (2016). β-glucan: crucial component of the fungal cell wall and elusive MAMP in plants. Fungal Genet. Biol. *90*, 53–60.

31. Wanke, A., Rovenich, H., Schwanke, F., Velte, S., Becker, S., Hehemann, J.-H., Wawra, S., and Zuccaro, A. (2020). Plant species-specific recognition of long and short β-1,3-linked glucans is mediated by different receptor systems. Plant J. *102*, 1142–1156.

32. Mélida, H., Sopeña-Torres, S., Bacete, L., Garrido-Arandia, M., Jordá, L., López, G., Muñoz-Barrios, A., Pacios, L.F., and Molina, A. (2018). Non-branched β-1,3-glucan oligosaccharides trigger immune responses in Arabidopsis. Plant J. *93*, 34–49.

33. Chandrasekar, B., Wanke, A., Wawra, S., Saake, P., Mahdi, L., Charura, N., Neidert, M., Poschmann, G., Malisic, M., Thiele, M., et al. (2022). Fungi hijack a ubiquitous plant apoplastic endoglucanase to release a ROS scavenging β-glucan decasaccharide to subvert immune responses. Plant Cell *34*, 2765–2784.

34. Martín-Dacal, M., Fernández-Calvo, P., Jiménez-Sandoval, P., López, G., Garrido-Arandía, M., Rebaque, D., Del Hierro, I., Berlanga, D.J., Torres, M.Á., Kumar, V., et al. (2023). Arabidopsis immune responses triggered by cellulose- and mixed-linked glucan-derived oligosaccharides require a group of leucine-rich repeat malectin receptor kinases. Plant J. *113*, 833–850.

35. Rebaque, D., Del Hierro, I., López, G., Bacete, L., Vilaplana, F., Dallabernardina, P., Pfrengle, F., Jordá, L., Sánchez-Vallet, A., Pérez, R., et al. (2021). Cell wall-derived mixed-linked β-1,3/1,4-glucans trigger immune responses and disease resistance in plants. Plant J. *106*, 601–615.

36. Barghahn, S., Arnal, G., Jain, N., Petutschnig, E., Brumer, H., and Lipka, V. (2021). Mixed linkage β-1,3/1,4-glucan oligosaccharides induce defense responses in Hordeum vulgare and Arabidopsis thaliana. Front. Plant Sci. *12*, 682439.

37. Kunze, G., Zipfel, C., Robatzek, S., Niehaus, K., Boller, T., and Felix, G. (2004). The N terminus of bacterial elongation factor Tu elicits innate immunity in Arabidopsis plants. Plant Cell *16*, 3496–3507.

38. Zipfel, C., Kunze, G., Chinchilla, D., Caniard, A., Jones, J.D.G., Boller, T., and Felix, G. (2006). Perception of the bacterial PAMP EF-Tu by the receptor EFR restricts Agrobacterium-mediated transformation. Cell *125*, 749–760.

39. Nizam, S., Qiang, X., Wawra, S., Nostadt, R., Getzke, F., Schwanke, F., Dreyer, I., Langen, G., and Zuccaro, A. (2019). Serendipita indica E5′NT modulates extracellular nucleotide levels in the plant apoplast and affects fungal colonization. EMBO Rep. *20*, e47430.

40. Umemoto, N., Kakitani, M., Iwamatsu, A., Yoshikawa, M., Yamaoka, N., and Ishida, I. (1997). The structure and function of a soybean beta-glucan-elicitor-binding protein. Proc. Natl. Acad. Sci. USA *94*, 1029–1034.

41. Sarkar, D., Rovenich, H., Jeena, G., Nizam, S., Tissier, A., Balcke, G.U., Mahdi, L.K., Bonkowski, M., Langen, G., and Zuccaro, A. (2019). The inconspicuous gatekeeper: endophytic Serendipita vermifera acts as extended plant protection barrier in the rhizosphere. New Phytol. *224*, 886–901.

42. Gol, L., Haraldsson, E.B., and von Korff, M. (2021). Ppd-H1 integrates drought stress signals to control spike development and flowering time in barley. J. Exp. Bot. *72*, 122–136.

43. Buscaill, P., Chandrasekar, B., Sanguankiattichai, N., Kourelis, J., Kaschani, F., Thomas, E.L., Morimoto, K., Kaiser, M., Preston, G.M., Ichinose, Y., and van der Hoorn, R.A.L. (2019). Glycosidase and glycan polymorphism control hydrolytic release of immunogenic flagellin peptides. Science *364*, eaav0748, https://doi.org/10.1126/science.aav0748.

44. Yu, X., Feng, B., He, P., and Shan, L. (2017). From chaos to harmony: responses and signaling upon microbial pattern recognition. Annu. Rev. Phytopathol. *55*, 109–137.

45. Fliegmann, J., Mithofer, A., Wanner, G., and Ebel, J. (2004). An ancient enzyme domain hidden in the putative beta-glucan elicitor receptor of soybean may play an active part in the perception of pathogen-associated molecular patterns during broad host resistance. J. Biol. Chem. *279*, 1132–1140.

46. Hilbert, M., Novero, M., Rovenich, H., Mari, S., Grimm, C., Bonfante, P., and Zuccaro, A. (2019). MLO differentially regulates barley root colonization by beneficial endophytic and mycorrhizal fungi. Front. Plant Sci. *10*, 1678.

47. Zuccaro, A., Lahrmann, U., Güldener, U., Langen, G., Pfiffi, S., Biedenkopf, D., Wong, P., Samans, B., Grimm, C., Basiewicz, M., et al. (2011). Endophytic life strategies decoded by genome and transcriptome analyses of the mutualistic root symbiont Piriformospora indica. PLoS Pathog. *7*, e1002290.

48. van Schie, C.C.N., and Takken, F.L.W. (2014). Susceptibility genes 101: how to be a good host. Annu. Rev. Phytopathol. *52*, 551–581.

49. Bravo, A., York, T., Pumplin, N., Mueller, L.A., and Harrison, M.J. (2016). Genes conserved for arbuscular mycorrhizal symbiosis identified through phylogenomics. Nat. Plants *2*, 15208.

50. Radhakrishnan, G.V., Keller, J., Rich, M.K., Vernié, T., Mbadinga Mbadinga, D.L., Vigneron, N., Cottret, L., Clemente, H.S., Libourel, C., Cheema, J., et al. (2020). An ancestral signalling pathway is conserved in intracellular symbioses-forming plant lineages. Nat. Plants *6*, 280–289.

51. Skiada, V., Avramidou, M., Bonfante, P., Genre, A., and Papadopoulou, K.K. (2020). An endophytic Fusarium-legume association is partially dependent on the common symbiotic signalling pathway. New Phytol. *226*, 1429–1444.

52. Wang, E., Schornack, S., Marsh, J.F., Gobbato, E., Schwessinger, B., Eastmond, P., Schultze, M., Kamoun, S., and Oldroyd, G.E.D. (2012). A common signaling process that promotes mycorrhizal and oomycete colonization of plants. Curr. Biol. *22*, 2242–2246.

53. Rey, T., Nars, A., Bonhomme, M., Bottin, A., Huguet, S., Balzergue, S., Jardinaud, M.-F., Bono, J.-J., Cullimore, J., Dumas, B., et al. (2013). NFP, a LysM protein controlling Nod factor perception, also intervenes in Medicago truncatula resistance to pathogens. New Phytol. *198*, 875–886.

54. Rey, T., Chatterjee, A., Buttay, M., Toulotte, J., and Schornack, S. (2015). Medicago truncatula symbiosis mutants affected in the interaction with a biotrophic root pathogen. New Phytol. *206*, 497–500.

55. Gobbato, E., Wang, E., Higgins, G., Bano, S.A., Henry, C., Schultze, M., and Oldroyd, G.E.D. (2013). RAM1 and RAM2 function and expression during arbuscular mycorrhizal symbiosis and Aphanomyces euteiches colonization. Plant Signal. Behav. *8*, e26049, https://doi.org/10.4161/psb.26049.

56. Ellinger, D., Naumann, M., Falter, C., Zwikowics, C., Jamrow, T., Manisseri, C., Somerville, S.C., and Voigt, C.A. (2013). Elevated early callose deposition results in complete penetration resistance to powdery mildew in Arabidopsis. Plant Physiol. *161*, 1433–1444.

57. Eggert, D., Naumann, M., Reimer, R., and Voigt, C.A. (2014). Nanoscale glucan polymer network causes pathogen resistance. Sci. Rep. *4*, 4159.

58. Ton, J., and Mauch-Mani, B. (2004). Beta-amino-butyric acid-induced resistance against necrotrophic pathogens is based on ABA-dependent priming for callose. Plant J. *38*, 119–130.

59. Skou, J.P., Jørgensen, J.H., and Lilholt, U. (1984). Comparative studies on callose formation in powdery mildew compatible and incompatible barley. J. Phytopathol. *109*, 147–168.

60. Jørgensen, I.H. (1992). Discovery, characterization and exploitation of Mlo powdery mildew resistance in barley. Euphytica *63*, 141–152.

61. Jacott, C.N., Charpentier, M., Murray, J.D., and Ridout, C.J. (2020). Mildew Locus O facilitates colonization by arbuscular mycorrhizal fungi in angiosperms. New Phytol. *227*, 343–351.

62. Jarosch, B., Kogel, K.-H., and Schaffrath, U. (1999). The ambivalence of the barley mlo locus: mutations conferring resistance against powdery mildew (Blumeria graminis f. sp. hordei) enhance susceptibility to the rice Blast Fungus Magnaporthe grisea. Mol. Plant Microbe Interact. *12*, 508–514.

63. McGrann, G.R.D., Stavrinides, A., Russell, J., Corbitt, M.M., Booth, A., Chartrain, L., Thomas, W.T.B., and Brown, J.K.M. (2014). A trade off between mlo resistance to powdery mildew and increased susceptibility of barley to a newly important disease, Ramularia leaf spot. J. Exp. Bot. *65*, 1025–1037.

64. Benedetti, M., Verrascina, I., Pontiggia, D., Locci, F., Mattei, B., De Lorenzo, G., and Cervone, F. (2018). Four Arabidopsis berberine bridge enzyme-like proteins are specific oxidases that inactivate the elicitor-active oligogalacturonides. Plant J. *94*, 260–273. https://doi.org/10.1111/tpj.13852.

65. Locci, F., Benedetti, M., Pontiggia, D., Citterico, M., Caprari, C., Mattei, B., Cervone, F., and De Lorenzo, G. (2019). An Arabidopsis berberine bridge enzyme-like protein specifically oxidizes cellulose oligomers and plays a role in immunity. Plant J. *98*, 540–554.

66. Dumas-Gaudot, E., Slezack, S., Dassi, B., Pozo, M.J., Gianinazzi-Pearson, V., and Gianinazzi, S. (1996). Plant hydrolytic enzymes (chitinases and β-1,3-glucanases) in root reactions to pathogenic and symbiotic microorganisms. Plant Soil *185*, 211–221.

67. Kelly, S., Hansen, S.B., Rübsam, H., Saake, P., Pedersen, E.B., Gysel, K., Madland, E., Wu, S., Wawra, S., Reid, D., et al. (2023). A glycan receptor kinase facilitates intracellular accommodation of arbuscular mycorrhiza and symbiotic rhizobia in the legume Lotus japonicus. PLoS Biol. *21*, e3002127.

68. Feng, F., Sun, J., Radhakrishnan, G.V., Lee, T., Bozsóki, Z., Fort, S., Gavrin, A., Gysel, K., Thygesen, M.B., Andersen, K.R., et al. (2019). A combination of chitooligosaccharide and lipochitooligosaccharide recognition promotes arbuscular mycorrhizal associations in Medicago truncatula. Nat. Commun. *10*, 5047.

69. Rush, T.A., Puech-Pagès, V., Bascaules, A., Jargeat, P., Maillet, F., Haouy, A., Maës, A.Q., Carriel, C.C., Khokhani, D., Keller-Pearson, M., et al. (2020). Lipo-chitooligosaccharides as regulatory signals of fungal growth and development. Nat. Commun. *11*, 3897.

70. Leclercq, J., Fliegmann, J., Tellström, V., Niebel, A., Cullimore, J.V., Niehaus, K., Küster, H., Ebel, J., and Mithöfer, A. (2008). Identification of a multigene family encoding putative beta-glucan-binding proteins in Medicago truncatula. J. Plant Physiol. *165*, 766–776.

71. Pang, Z., Otaka, K., Maoka, T., Hidaka, K., Ishijima, S., Oda, M., and Ohnishi, M. (2005). Structure of beta-glucan oligomer from laminarin and its effect on human monocytes to inhibit the proliferation of U937 cells. Biosci. Biotechnol. Biochem. *69*, 553–558.

72. Mystkowska, A.A., Robb, C., Vidal-Melgosa, S., Vanni, C., Fernandez-Guerra, A., Höhne, M., and Hehemann, J.-H. (2018). Molecular recognition of the beta-glucans laminarin and pustulan by a SusD-like glycan-binding protein of a marine Bacteroidetes. FEBS Journal *285*, 4465–4481.

73. Perez-Riverol, Y., Csordas, A., Bai, J., Bernal-Llinares, M., Hewapathirana, S., Kundu, D.J., Inuganti, A., Griss, J., Mayer, G., Eisenacher, M., et al. (2019). The PRIDE database and related tools and resources in 2019: improving support for quantification data. Nucleic Acids Res. *47*, D442–D450.

74. Hinze, K., Thompson, R.D., Ritter, E., Salamini, F., and Schulze-Lefert, P. (1991). Restriction fragment length polymorphism-mediated targeting of the ml-o resistance locus in barley (Hordeum vulgare). Proc. Natl. Acad. Sci. USA *88*, 3691–3695.

75. Mahdi, L.K., Miyauchi, S., Uhlmann, C., Garrido-Oter, R., Langen, G., Wawra, S., Niu, Y., Guan, R., Robertson-Albertyn, S., Bulgarelli, D., et al. (2022). The fungal root endophyte Serendipita vermifera displays inter-kingdom synergistic beneficial effects with the microbiota in Arabidopsis thaliana and barley. ISME J. *16*, 876–889.

76. Deshmukh, S., Hückelhoven, R., Schäfer, P., Imani, J., Sharma, M., Weiss, M., Waller, F., and Kogel, K.-H. (2006). The root endophytic fungus Piriformospora indica requires host cell death for proliferation during mutualistic symbiosis with barley. Proc. Natl. Acad. Sci. USA *103*, 18450–18457.

77. Schäfer, P., Pfiffi, S., Voll, L.M., Zajic, D., Chandler, P.M., Waller, F., Scholz, U., Pons-Kühnemann, J., Sonnewald, S., Sonnewald, U., and Kogel, K.-H. (2009). Manipulation of plant innate immunity and gibberellin as factor of compatibility in the mutualistic association of barley roots with Piriformospora indica. Plant J. *59*, 461–474.

78. Witte, C.-P., Noël, L.D., Gielbert, J., Parker, J.E., and Romeis, T. (2004). Rapid one-step protein purification from plant material using the eight-amino acid StrepII epitope. Plant Mol. Biol. *55*, 135–147.

79. Myrach, T., Zhu, A., and Witte, C.-P. (2017). The assembly of the plant urease activation complex and the essential role of the urease accessory protein G (UreG) in delivery of nickel to urease. J. Biol. Chem. *292*, 14556–14565.

80. Concordet, J.-P., and Haeussler, M. (2018). CRISPOR: intuitive guide selection for CRISPR/Cas9 genome editing experiments and screens. Nucleic Acids Res. *46*, W242–W245.

81. Schneider, C.A., Rasband, W.S., and Eliceiri, K.W. (2012). NIH Image to ImageJ: 25 years of image analysis. Nat. Methods *9*, 671–675.

82. Lahrmann, U., Ding, Y., Banhara, A., Rath, M., Hajirezaei, M.R., Döhlemann, S., von Wirén, N., Parniske, M., and Zuccaro, A. (2013). Host-related metabolic cues affect colonization strategies of a root endophyte. Proc. Natl. Acad. Sci. USA *110*, 13965–13970.

83. Vierheilig, H., Coughlan, A.P., Wyss, U., and Piche, Y. (1998). Ink and vinegar, a simple staining technique for arbuscular-mycorrhizal fungi. Appl. Environ. Microbiol. *64*, 5004–5007.

84. Werner, A.K., Sparkes, I.A., Romeis, T., and Witte, C.-P. (2008). Identification, biochemical characterization, and subcellular localization of allantoate amidohydrolases from Arabidopsis and soybean. Plant Physiol. *146*, 418–430.

85. Felix, G., Duran, J.D., Volko, S., and Boller, T. (1999). Plants have a sensitive perception system for the most conserved domain of bacterial flagellin. Plant J. *18*, 265–276.

86. Günl, M., Kraemer, F., and Pauly, M. (2011). Oligosaccharide mass profiling (OLIMP) of cell wall polysaccharides by MALDI-TOF/MS. Methods Mol. Biol. *715*, 43–54.

87. Kumar, N., Galli, M., Ordon, J., Stuttmann, J., Kogel, K.-H., and Imani, J. (2018). Further analysis of barley MORC1 using a highly efficient RNA-guided Cas9 gene-editing system. Plant Biotechnol. J. *16*, 1892–1903.

88. Amanda, D., Frey, F.P., Neumann, U., Przybyl, M., Šimura, J., Zhang, Y., Chen, Z., Gallavotti, A., Fernie, A.R., Ljung, K., and Acosta, I.F. (2022). Auxin boosts energy generation pathways to fuel pollen maturation in barley. Curr. Biol. *32*, 1798–1811.e8.

89. Mason, K.N., Ekanayake, G., and Hesse, A. (2020). Staining and automated image quantification of callose in Arabidopsis cotyledons and leaves. Methods Cell Biol. *160*, 181–199.

STAR★METHODS

KEY RESOURCES TABLE

REAGENT or RESOURCE	SOURCE	IDENTIFIER
Bacterial and virus strains		
Escherichia coli MachI	University of Cologne, Germany (Prof. Dr. Ute Hoecker)	N/A
Agrobacterium tumefaciens GV3101::pMP90RK	this paper	N/A
Agrobacterium tumefaciens GV3101::pBIN61-p19	this paper	N/A
Chemicals, peptides, and recombinant proteins		
Horseradish peroxidase	Sigma-Aldrich	P6782; CAS: 9003-99-0
L-012	Wako Chemicals	120-04891; CAS: 143556-24-5
Rifampicin	Roth	4163.2; CAS: 13292-46-1
Kanamycin	Duchefa	K0126.0010; CAS: 25389-94-0
Carbenicillin	Roth	6344.1; CAS: 4800-94-6
Gentamicin	Roth	0233.2; CAS: 1405-41-0
Sodium hypochlorite	Roth	9062.4; CAS: 7681-52-9
T4 polynucleotide kinase	New England BioLabs	CAT#M0201S
T4 DNA ligase	New England BioLabs	CAT#M0202M
DpnI	New England BioLabs	CAT#R0176L
T4 DNA ligase buffer	New England BioLabs	CAT#B0202S
N-naphthol	Sigma Aldrich	N1000-10G; CAS: 90-15-3
D-glucose	Roth	6887.2; CAS: 77938-63-7
Laminaribiose β-1-3-$(Glc)_2$	Megazyme	O-LAM2; CAS: 34980-39-7
Laminaritriose β-1-3-$(Glc)_3$	Megazyme	O-LAM3; CAS: 3256-04-0
Laminaripentaose β-1-3-$(Glc)_5$	Megazyme	O-LAM5; CAS: 23743-55-7
Gentiobiose β-1-6-$(Glc)_2$	Megazyme	O-GENT; CAS: 554-91-6
endo-1,3-β-D-glucanase (barley BGLUII)	Megazyme	E-LAMHV; CAS: 9025-37-0
Chitohexaose	Megazyme	O-CHI6; CAS: 38854-46-5
Cellohexaose	Megazyme	O-CHE; CAS: 2478-35-5
Xyloglucan oligomer (XXXG)	Megazyme	O-X3G4; CAS: 121591-98-8
Laminarin from *Eisenia bicyclis*	Biosynth	YL02421; CAS: 9008-22-4
Laminarin from *Laminaria digitata*	Sigma Aldrich	L9634-1G; CAS: 9008-22-4
Elf18	The Sainsbury Laboratory, United Kingdom (Prof. Dr. Cyril Zipfel)	N/A
EZ-Link Hydrazide-Biotin	Thermo Scientific	CAT#21339
Sodium cyanoborohydride	Sigma Aldrich	42077-10G; CAS: 25895-60-7
Aniline blue	Sigma Aldrich	415049-25G; CAS: 666787-07-8
Concanavalin A (ConA) - Alexa Fluor 633	Invitrogen, Thermo Fisher Scientific	CAT#C21402
Wheat Germ Agglutinin (WGA) - Alexa Fluor 488	Invitrogen, Thermo Fisher Scientific	CAT#W11261
Avidin	Sigma Aldrich	A9275-5MG; CAS: 1405-69-2
Acetosyringone	Roth	6003.2; CAS: 2478-38-8
NeutrAvidin agarose resin	Thermo Fisher Scientific	CAT#29200
Blue ink	Pelikan	301010
Gelrite	Duchefa	G1101; CAS: 71010-52-1
Strep-Tactin Macroprep	IBA Lifesciences GmbH	2-1505-010
Critical commercial assays		
NucleoSpin Gel and PCR Clean-up Kit	Macherey-Nagel	740609.50
NucleoSpin Plasmid Kit	Macherey-Nagel	740588.50

(*Continued on next page*)

Continued

REAGENT or RESOURCE	SOURCE	IDENTIFIER
Deposited data		
Proteomic data	ProteomeXchange Consortium via PRIDE partner repository (Perez-Riverol et al.[73])	PXD046129
Experimental models: Organisms/strains		
Serendipita indica: DSM11827	German Collection of Microorganisms and Cell Cultures (DSMZ)	NCBI Taxonomy ID: 1109443
Serendipita vermifera: MAFF305830	NARO Research Center of Genetic Resources, Japan	NCBI Taxonomy ID: 933852
Bipolaris sorokiniana: ND90Pr	Max Planck Institute for Terrestrial Microbiology, Marburg, Germany (Shadab Nizam)	NCBI Taxonomy ID: 665912
Blumeria hordei: K1	Hinze et al.[74]	NCBI Taxonomy ID: 1283759
Rhizophagus irregularis: DAOM197198	Symplanta	00101SP; https://www.symplanta.com/productcatalog.html
Barley: control: *Hordeum vulgare* (cv. Golden Promise Fast)	Gol et al.[42]	N/A
Barley: *gbp1 gbp2 #1*: *Hordeum vulgare* (cv. Golden Promise Fast) *gbp1-1 gbp2-1*	this paper	N/A
Barley: *gbp1 gbp2 #2: Hordeum vulgare* (cv. Golden Promise Fast) *gbp1-2 gbp2-2/gbp2-3*	this paper	N/A
Nicotiana benthamiana	The Sainsbury Laboratory, United Kingdom (Prof. Dr. Cyril Zipfel)	N/A
Oligonucleotides		
Primers for cloning see Table S1	this paper	N/A
Primers for site-directed mutagenesis see Table S1	this paper	N/A
Primers for CRISPR/Cas9 gRNA see Table S1	this paper	N/A
Primers for *S. indica* colonization assay (qPCR) see Table S1	Chandrasekar et al.[33]	N/A
Primers for *S. vermifera* colonization assay (qPCR) see Table S1	Mahdi et al.[75]	N/A
Primers for *B. sorokiniana* colonization assay (qPCR) see Table S1	Mahdi et al.[75]	N/A
Primers for *H. vulgare* colonization assay (qPCR) see Table S1	Deshmukh et al.[76]	Accession no. M60175
Primers for barley *PR10* expression (qPCR) see Table S1	Schäfer et al.[77]	N/A
Recombinant DNA		
pXCScpmv-HAStrep	Witte et al.[78]; Myrach et al.[79]	N/A
pXCScpmv-GBP1-HAStrep	This paper	N/A
pXCScpmv-GBP1_E500A-HAStrep	This paper	N/A
pMGE625	Martin Luther University Halle-Wittenburg, Germany (Prof. Dr. Johannes Stuttmann)	N/A
pMGE626	Martin Luther University Halle-Wittenburg, Germany (Prof. Dr. Johannes Stuttmann)	N/A
pMGE628	Martin Luther University Halle-Wittenburg, Germany (Prof. Dr. Johannes Stuttmann)	N/A
pMGE629	Martin Luther University Halle-Wittenburg, Germany (Prof. Dr. Johannes Stuttmann)	N/A
pMGE599	Martin Luther University Halle-Wittenburg, Germany (Prof. Dr. Johannes Stuttmann)	N/A

(*Continued on next page*)

Continued

REAGENT or RESOURCE	SOURCE	IDENTIFIER
pMP202	Martin Luther University Halle-Wittenburg, Germany (Prof. Dr. Johannes Stuttmann)	N/A
Software and algorithms		
Flexanalysis software (v. 4.0)	Bruker Daltonics	https://www.bruker.com/en.html
CRISPOR web tool (v. 4.97)	Concordet and Haeussler[80]	http://crispor.tefor.net/
ImageJ (v. 1.53)	Schneider et al.[81]	https://imagej.nih.gov/ij/
SparkControl (v. 2.1)	Tecan	https://lifesciences.tecan.com/multimode-plate-reader?p=tab–3
Scaffold (v. 4)	Proteome Software	https://www.proteomesoftware.com/products/scaffold-5
MSConvert package	ProteoWizard	https://proteowizard.sourceforge.io/download.html
Mascot server (v. 2.3)	Matrix Science	https://www.matrixscience.com/server.html
Other		
TECAN SPARK 10 M multiwell plate reader	Tecan	N/A
PD MidiTrap G-10 column	Cytiva	28918011
TCS SP8 confocal microscope	Leica	https://www.leica-microsystems.com/
AxioStar light microscope	Carl Zeiss	N/A
Silica gel 60 F254 aluminum TLC plate	Merck Millipore	105554
MALDI-TOF mass spectrometer (rapifleX instrument)	Bruker	https://www.bruker.com/en/products-and-solutions/mass-spectrometry/maldi-tof/rapiflex.html
Reverse phase trap column (Acclaim PepMap, C18 5 μm, 100 μm x 2 cm)	Thermo Scientific	N/A
Analytical column (Acclaim PepMap 100, C18 3 μm, 75 μm x 50 cm)	Thermo Scientific	CAT#164570
Orbitrap Fusion Tribrid mass spectrometer	Thermo Scientific	https://www.thermofisher.com/de/de/home/industrial/mass-spectrometry/liquid-chromatography-mass-spectrometry-lc-ms/lc-ms-systems/orbitrap-lc-ms/orbitrap-tribrid-mass-spectrometers.html#fusion-tribrid
Nanoflow-UHPLC system (UltiMate3000 Dionex)	Thermo Scientific	N/A
PD-10 desalting column	Sigma Aldrich	GE17-0851-01

RESOURCE AVAILABILITY

Lead Contact

Further information and requests for resources, reagents, datasets, and protocols should be directed to and will be fulfilled by the lead contact, Alga Zuccaro (azuccaro@uni-koeln.de).

Materials Availability

Plasmids and barley lines generated in this study are available upon request and will be provided by the lead contact, Alga Zuccaro (azuccaro@uni-koeln.de).

Data and Code Availability

- Proteomic data has been deposited at the ProteomeXchange Consortium via PRIDE partner repository[73] and are publicly available as of the date of publication. Accession numbers are listed in the key resources table.
- This paper does not report original code.
- Any additional information required to reanalyze the data reported in this paper is available from the lead contact upon request.

EXPERIMENTAL MODEL AND SUBJECT DETAILS

Plant material and growth conditions

Hordeum vulgare

All experiments, including the generation of CRISPR/Cas9 knock-out lines, were performed with the spring barley (*H. vulgare* L.) cv. Golden Promise Fast, an introgression line carrying the *Ppd-H1* allele that confers fast flowering.[42] From here on, we use "control" to name this non-mutagenized cultivar that carries normal copies of *GBP1* and *GBP2*. For ROS burst assays, barley seeds were surface sterilized with 6% sodium hypochlorite for 1 h and then washed extensively (5 × 30 mL sterile water). Seeds were germinated on wet filter paper at room temperature in the dark under sterile conditions for three days before transfer to sterile jars containing solid 1/10 plant nutrition medium (PNM), pH 5.7 and 0.4% Gelrite (Duchefa, Haarlem, the Netherlands).[82] Seedlings were cultured for four days in a growth chamber under long-day conditions (day/night cycle of 16/8 h, 22 °C/18 °C, light intensity of 108 $\mu mol \cdot m^{-2} \cdot s^{-1}$).

Nicotiana benthamiana

Seeds of *N. benthamiana* wild-type lines were sown on soil and grown for 3 weeks in the greenhouse under long-day conditions (day/night cycle of 16/8 h, 22–25 °C, light intensity of ~140 $\mu mol \cdot m^{-2} \cdot s^{-1}$, maximal humidity of 60%).

Fungal material, growth conditions and barley colonization assays

Serendipita indica, Serendipita vermifera *and* Bipolaris sorokiniana

The growth conditions for barley, *S. indica* (DSM11827, Si), *S. vermifera* (MAFF305830, Sv) and *B. sorokiniana* (ND90Pr, Bs) and the preparation of fungal suspensions for plant inoculation have been described previously.[41,75] Four-day-old barley seedlings were transferred to sterile jars on 1/10 PNM (pH 5.7) and inoculated with 3 mL of either sterile water as control, *Si* chlamydospores (500,000 spores $\cdot mL^{-1}$), *Sv* mycelium (1 g per 50 mL), or *Bs* conidia (5,000 spores $\cdot mL^{-1}$). Plants were grown on a day/night cycle of 16/8 h at 22/18 °C and 60% humidity under a light intensity of 108 $\mu mol \cdot m^{-2} \cdot s^{-1}$. Plant roots were harvested six days post inoculation (dpi), washed thoroughly to remove extraradical fungal hyphae, and frozen in liquid nitrogen. Four barley plants were pooled per biological replicate. To quantify fungal colonization and *PR10* gene expression, RNA extraction, cDNA generation and RT-PCR were performed as previously described.[41]

Blumeria hordei *(formerly* Blumeria graminis *f. sp.* hordei*)*

Blumeria hordei isolate K1[74] was maintained on intact plants of barley cv. Golden Promise grown in soil at 19 °C, 60% relative humidity and a photoperiod of 14 h with a light intensity of 100 $\mu mol \cdot m^{-2} s^{-1}$. Control and *GBP* knock-out lines were grown in soil in a growth chamber (poly klima) at 19 °C, 60% relative humidity and a photoperiod of 14 h with a light intensity of 100 $\mu mol \cdot m^{-2} \cdot s^{-1}$. Primary leaves of seven-day-old plants were cut and placed with the adaxial side down on 1% plant agar plates before gravity inoculation with *B. hordei* isolate K1 at a conidial density of about 20 conidia per mm. Leaves were harvested at 48 h and cleared in 70% ethanol before staining of the fungal structures with Coomassie brilliant blue solution (0.1% [w/v] Coomassie brilliant blue R-250 in 50% ethanol and 10% acetic acid) for 10-15 s. Bright field microscopy was used to assess secondary hyphae formation in 50 germinated conidia spores in the tip area and 50 germinated conidia in the middle of the leaf. At least six independent leaves were examined at 48 h after infection for fungal penetration success.

Rhizophagus irregularis

Barley control and mutant seeds were sterilized and germinated as described previously.[75] Germinated seedlings were transferred to 9 × 9 cm pots containing autoclaved 1:1 silica sand:vermiculite mixture inoculated with 700 mg *R. irregularis* spore inoculum (10,000 spores $\cdot g^{-1}$ moist diatomaceous earth powder [50% water]) (Symplanta, Darmstadt, Germany). Approximately 500 mg of the inoculum was evenly mixed into the lower two-third substrate layer, further 200 mg were evenly sprinkled into a hole in the upper third of the substrate layer, into which the seedlings were transplanted. The seedlings were grown in the greenhouse and watered weekly with 30 mL of deionized water and tap water in a 1:1 ratio. Roots were harvested at 28 dpi and stored in 50% EtOH at 4 °C until staining.

Roots were stained according to a previously published protocol.[83] Briefly, roots were incubated for 15 min at 95 °C in 10% KOH, washed with 10% acetic acid and incubated for 5 min at 95 °C with a staining solution of 5% ink (Pelikan, Falkensee, Germany) in 5% acetic acid. After staining, the roots were carefully washed with tap water, then incubated in 5% acetic acid at 4 °C for at least 20 min. The ink-stained root tissue was cut into 1 cm segments with a scalpel and 30 segments of similar diameter were randomly selected from each genotype. Cross-section points were determined from 10 random cuts per root segment. Ink-stained *R. irregularis* structures such as intraradical hyphae (IRH), extraradical hyphae (ERH), arbuscules and vesicles were visualized with a light microscope (AxioStar, Carl Zeiss, Jena, Germany) at 10× magnification. Colonization with *R. irregularis* was scored as positive if IRH, arbuscules or vesicles were present. The roots of four biological replicates per genotype were examined.

METHOD DETAILS

Carbohydrate substrates for immunity and enzymatic digestion assays

All laminarioligomeres, gentiobiose, chitohexaose, cellohexaose and xyloglucan oligomer (XXXG) were purchased from Megazyme (Bray, Ireland). Laminarin from *Laminaria digitata* was purchased from Sigma-Aldrich (Taufkirchen, Germany) and laminarin from *Eisenia bicyclis* was purchased from Biosynth (Staad, Switzerland). Substrates derived from *S. indica* CW and EPS matrix were purified and prepared as previously described.[33]

Identification of protein candidates interacting with β-glucan

Biotinylation of laminarin

Laminarin (final concentration ~ 60 mM) was incubated with biotin-hydrazide (120 mM) and sodium cyanoborohydride (1 M) for 2 h at 65 °C. The product was purified on a PD MidiTrap G-10 column (GE Healthcare) according to the manufacturer's description. Success of biotinylation was validated via mass spectrometry. The immunogenic capacity of biotinylated laminarin was confirmed via ROS burst assays.

Protein pull-down with biotinylated laminarin

Barley leaves from 2-week-old plants were treated for 15 min with biotinylated laminarin, followed by vacuum infiltration for 2 min. Untreated laminarin and a biotinylated version of the bacterial elongation factor Tu peptide (elf18) were used as controls. The tissue was frozen in liquid nitrogen and ground to fine powder. Then, 10 mg·mL^{-1} of extraction buffer (10 mM MES, 50 mM NaCl, 10 mM $MgCl_2$, 1 mM DTT, 1% IGEPAL, proteinase inhibitor cocktail) were added to the powder. To avoid pH-dependent binding effects to the NeutrAvidin beads, two buffer conditions (pH 5.6 and pH 8.0) were used for all treatments. Samples were incubated rotating at 4 °C for 60 min and centrifuged at 10,645 *g*, 4 °C for 15 min. Supernatant was filtered to remove pieces, mixed with 50 μL of high-capacity NeutrAvidin agarose resin (Thermo Fisher Scientific, Schwerte, Germany), and incubated (inverting) at 4 °C for 3 h. The sample was briefly centrifuged at 60 *g* for 1 min. After discarding the supernatant, the beads were washed four times with 10 mL of wash buffer (10 mM MES [pH 5.6 or pH 8.0], 50 mM NaCl, 10 mM $MgCl_2$, 0.5% IGEPAL). Proteins were eluted by boiling the beads with 50-70 μL of 2x SDS loading (including reducing agent) for 5 min. Proteins were separated by SDS-PAGE (NuPAGE; Invitrogen, Waltham, United States) after staining with Coomassie brilliant blue G-250, cut out for mass spectrometric analysis and digested with trypsin.

Tandem mass spectrometric (MS-MS) analysis of the pull-down proteins

LC-MS/MS analysis was performed using an Orbitrap Fusion tribrid mass spectrometer (Thermo Scientific) and a nanoflow-UHPLC system (Dionex UltiMate3000, Thermo Scientific). Peptides were trapped to a reverse phase trap column (Acclaim PepMap, C18 5 μm, 100 μm x 2 cm, Thermo Scientific) connected to an analytical column (Acclaim PepMap 100, C18 3 μm, 75 μm x 50 cm, Thermo Scientific). Peptides were eluted in a gradient of 3-40% acetonitrile in 0.1% formic acid (solvent B) over 86 min followed by gradient of 40-80% B over 6 min at a flow rate of 200 nL·min at 40 °C. The mass spectrometer was operated in positive ion mode with nano-electrospray ion source with ID 0.02mm fused silica emitter (New Objective). Voltage +2200 V was applied via platinum wire held in PEEK T-shaped coupling union with transfer capillary temperature set to 275 ºC. The Orbitrap, MS scan resolution of 120,000 at 400 *m/z*, range 300 to 1800 *m/z* was used, and automatic gain control (AGC) was set at 2e5 and maximum injection time to 50 ms. In the linear ion trap, MS/MS spectra were triggered with a data dependent acquisition method using 'top speed' and 'most intense ion' settings. The selected precursor ions were fragmented sequentially in both the ion trap using CID and in the HCD cell. Dynamic exclusion was set to 15 s. Charge state allowed between 2+ and 7+ charge states to be selected for MS/MS fragmentation. Peak lists in the format of Mascot generic files (mgf files) were prepared from raw data using MSConvert package (ProteoWizard). Peak lists were searched on Mascot server v.2.3 (Matrix Science) against a *Hordeum vulgare* Morex v1.0 database (IBSC_v2, IPK Gatersleben) and an in-house contaminants database. Tryptic peptides with up to two possible mis-cleavages and charge states +2, +3, +4, were allowed in the search. The following modifications were included in the search: oxidized methionine as variable modification and carbamidomethylated cysteine as static modification. Data were searched with a monoisotopic precursor and fragment ions mass tolerance 10 ppm and 0.6 Da, respectively. Mascot results were combined in Scaffold v. 4 (Proteome Software) and exported in Excel (Microsoft Office, Table S1).

Plasmid construction for the heterologous expression of barley GBP1 in *N. benthamiana*

For *in planta* protein production in *N. benthamiana*, we used the binary vector pXCScpmv-HAStrep characterized by a 35S promoter cassette, modified 5′- and 3′-UTRs of RNA-2 from the cowpea mosaic virus as translational enhancers, and C-terminal hemagglutinin (HA) and StrepII tags.[78,79] The codon-optimized GBP1 coding sequence was amplified with the primer pair *ClaI*_GBP1_F (5'-gacgg tatcgataaaATGCCGCCACATGGTAGACG-3') and GBP1_noSTOP_*XmaI*_R (5'-ataactcccgggATGGCCATATTGACGATACCAA CAGC-3') and directionally cloned into the *ClaI* and *XmaI* sites of the binary vector to produce pXCScpmv-GBP1-HAStrep. To generate a catalytically inactive version of GBP1, the first glutamate residue of the catalytic center (E500) was exchanged to an alanine residue via site-directed mutagenesis PCR with the primer pair GBP1_E500A_F (5'-CAGGCATCAACATCAGAAGCAGTG-3') and GBP1_E500A_R (5'-GTTCCTACCATCTCCAAACTCAGTC-3'). The linearized, mutated plasmid was purified after gel electrophoresis using the NucleoSpin Gel and PCR Clean-up Kit (Macherey-Nagel, Düren, Germany). The isolated DNA fragment was treated with a self-made KLD mixture (1,000 units·mL^{-1} T4 polynucleotide kinase, 40,000 T4 DNA ligase units·mL^{-1} ligase 2,000 units·mL^{-1} DpnI, 1 × T4 DNA ligase buffer; all enzymes were purchased from New England BioLabs, Ipswich, USA) for 1 h at room temperature before transformation into *Escherichia coli* MachI cells. Plasmids were isolated using the NucleoSpin Plasmid Kit (Machery-Nagel, Düren, Germany) and sequenced to confirm the introduced mutation. Both plasmids (pXCScpmv-GBP1-HAStrep and pXCScpmv-GBP1_E500A-HAStrep) were introduced into *Agrobacterium tumefaciens* GV3101::pMP90RK strains for transient transformation of *N. benthamiana* leaf tissue.

Heterologous protein production and purification from *N. benthamiana*

A. tumefaciens GV3101::pMP90RK strains carrying the binary vectors for protein production (antibiotic selection: 30 μg·mL^{-1} Rifampicin, 25 μg·mL^{-1} Kanamycin, 50 μg·mL^{-1} Carbenicillin) and *A. tumefaciens* GV3101 strains carrying the binary vector for viral p19 silencing inhibitor expression (antibiotic selection: 30 μg·mL^{-1} Rifampicin, 30 μg·mL^{-1} Gentamicin, 100 μg·mL^{-1} Carbenicillin)

were grown in selection LB liquid medium at 28 °C, 180 rpm for three days. The cultures were centrifuged (3,500 *g* for 15 min), re-suspended in infiltration buffer (10 mM MES pH 5.5, 10 mM $MgCl_2$, 200 μM acetosyringone) to an OD_{600} of 1 and incubated for 1 h in the dark at 28 °C, 180 rpm. Each of the two *A. tumefaciens* strains carrying the GBP1 production constructs was mixed with the *A. tumefaciens* strain carrying the p19-expressing construct in a 1:1 ratio. The bacterial suspensions were infiltrated into the four youngest, fully developed leaves of four-week-old *N. benthamiana* plants with a needleless syringe. Five days after infiltration, the leaves were detached from the plant and ground in liquid nitrogen. Protein purification was carried out according to Werner and co-workers[84] with minor modifications: The ground plant material (up to the 5 mL mark of 15-mL tube) was thoroughly resuspended in 5 mL of ice-cold extraction buffer (100 mM Tris pH 8.0, 100 mM NaCl, 5 mM EDTA, 0.5% Triton X-100, 10 mM DTT, 100 $\mu g \cdot mL^{-1}$ Avidin) and centrifuged at 10,000 *g*, 4 °C for 10 min. The supernatant was filtered through a PD-10 desalting column (Sigma-Aldrich, Taufkirchen, Germany), transferred to a new tube, and supplemented with 75 $\mu L \cdot mL^{-1}$ Strep-Tactin Macroprep (50% slurry) (IBA Lifesciences GmbH, Göttingen, Germany). Samples were incubated in a rotary wheel at 4 °C for 1 h, followed by centrifugation for 30 s at 700 *g*. The supernatant was discarded, and the beads were washed three times with 2 mL of washing buffer (50 mM Tris pH 8.0, 100 mM NaCl, 0.5 mM EDTA, 0.005% Triton X-100, 2 mM DTT). Proteins were eluted from the beads by adding 100 μL of elution buffer (wash buffer containing 10 mM biotin) and incubating at 800 rpm for 5 min at 25 °C. The samples were centrifuged at 700 *g* for 20 s and the elution was repeated two more times. The elution fractions were pooled and dialyzed overnight against cold Milli-Q water (dialysis tubing with 6-8 kDa cut-off). Proteins were stored on ice at 4 °C for further use. The success of protein purification was analyzed by SDS PAGE and Western Blotting.

Oxidative burst assay

Preparation of the plant material

For immunity assays in barley, the roots and shoots of seven-day-old seedlings were separated. The root tissue between 2 cm below the seed and 1 cm above the tip was cut into 5 mm pieces. Each assay was carried out with randomly selected root pieces from 16 barley seedlings. Four root pieces were transferred to each well of a 96-well microtiter plate containing 150 μL of sterile Milli-Q water. Barley shoot assays were performed on 3-mm leaf discs punched from the youngest leaves of eight individual barley seedlings.

For immunity assays in *N. benthamiana*, 3-mm leaf discs from the youngest, fully developed leaf of eight three-week-old plants were transferred to a 96-well plate filled with 150 μL of sterile Milli-Q water.

Assay protocol

The ROS burst assay was based on previously published protocols.[33,85] In brief, a 96-well plate containing water and plant material (as described above) was incubated overnight at RT to remove ROS that had resulted from mechanical damage to the tissue during preparation. The next day, the water was replaced with 100 μL of fresh Milli-Q water containing 20 $\mu g \cdot mL^{-1}$ horseradish peroxidase (Sigma-Aldrich, Taufkirchen, Germany) and 20 μM L-012 (Wako Chemicals, Neuss, Germany). After a short incubation period (~15 min), 100 μL of double-concentrated elicitor solutions were added to the wells. All elicitors were dissolved in Milli-Q water without additional treatment. Measurements of elicitor-triggered apoplastic ROS production were started immediately and performed continuously with an integration time of 450 ms in a TECAN SPARK 10 M multiwell plate reader (Männedorf, Switzerland).

Enzymatic carbohydrate digestion and thin layer chromatography (TLC)

Carbohydrate digestion assays were performed using either purified barley GBP (heterologously expressed in *N. benthamiana*) or barley BGLUII[33] (available from Megazyme, E-LAMHV). Preparations of the fungal CW and EPS matrix were incubated overnight in sterile Milli-Q water at 65 °C prior to enzymatic digestion. Substrate and enzyme concentrations, buffer compositions, digestion temperature and time are described in the figure captions. Digestion was stopped by denaturing the enzymes at 95 °C for 10 min and the digestion products were stored at -20 °C prior to use. An aliquot of each sample was subjected to TLC using a silica gel 60 F254 aluminum TLC plate (Merck Millipore, Burlington, USA), using a running buffer containing ethyl acetate/acetic acid/methanol/formic acid/water at a ratio of 8:4:1:1:1 (v/v). D-glucose, laminaribiose β-1-3-$(Glc)_2$, laminaritriose β-1-3-$(Glc)_3$, gentiobiose β-1-6-$(Glc)_2$, and laminaripentaose β-1-3-$(Glc)_5$ at a concentration of 1.5 $mg \cdot mL^{-1}$ were used as standards (Megazyme, Bray, Ireland). To visualize the glucan fragments, the TLC plate was sprayed with glucan developer solution (45 mg N-naphthol, 4.8 mL H_2SO_4, 37.2 mL ethanol and 3 mL water) and baked at 95 °C until the glucan bands became visible (approximately 4-5 min).

MALDI-TOF analysis

The digested products of GBP1 were analyzed using Oligosaccharide Mass Profiling as previously described.[86] Briefly, 2 μL of the samples were spotted onto 2 μL of crystalized dihydroxy benzoic acid matrix (10 $mg \cdot mL^{-1}$) and analyzed by MALDI-TOF mass spectrometry (Bruker rapifleX instrument, Bremen). Mass spectra were recorded in linear positive reflectron mode with an accelerating voltage of 20,000 V. The spectra of the samples were analyzed using the flexanalysis software 4.0 (Bruker Daltonics, Billerica, USA).

CRISPR/Cas9-based mutagenesis of GBP homologues in barley

The CRISPOR web tool[80] (version 4.97) was used to design two single guide RNAs for each *GBP1* and *GBP2*:

GBP1_gRNA1: 5'-CCCGGCACGCTTCTTCGCGCCGG-3'
GBP1_gRNA2: 5'-TGGCGCCTTCGGATGAACAGCGG-3'
GBP2_gRNA1: 5'-TAAGATCCGTCGAGGCAGTATGG-3'
GBP2_gRNA2: 5'-GTACAGCCGTTGCTACCCGACGG-3'

Golden Gate cloning was used to load each guide sequence from complementary oligonucleotides into shuttle vectors pMGE625, pMGE626, pMGE628, pMGE629. The four guide expression cassettes were then assembled into binary vector pMGE599 to create pMP202. Vectors and cloning protocols have been previously described[87] and were kindly provided by Johannes Stuttmann. Stable transformation of pMP202 in cv. Golden Promise Fast was performed as previously described.[88]

Staining for confocal microscopy

Root tissue of barley control and mutant plants colonized by *S. indica* was harvested at 6 dpi and then stained as previously described.[46] Briefly, roots were incubated at 95 °C for 2 min in 10% KOH, washed 3 times for 30 min in deionized water and 3 times for 30 min in PBS (pH 7.4). The roots were stained for 5 min under vacuum and then washed three times with deionized water. Fungal structures were visualized using 10 $\mu g \cdot mL^{-1}$ fluorescently labeled wheat germ agglutinin (WGA-AF488, Invitrogen, Thermo Fisher Scientific, Schwerte, Germany) in PBS (pH 7.4) and imaging was conducted with an excitation wavelength of 488 nm and emission detection between 500-540 nm. Papillae and root cell wall appositions were stained with 10 $\mu g \cdot mL^{-1}$ fluorescently labeled Concanavalin A (ConA-AF633, Invitrogen, Thermo Fisher Scientific, Schwerte, Germany) in PBS (pH 7.4) and imaged by excitation at 633 nm and detection at 650-690 nm.

Callose was stained by aniline blue according to a protocol adapted from Mason and coworkers.[89] Roots were incubated at 95 °C for 2 min in 10% KOH, washed 3 times for 30 min in deionized water and 3 times for 30 min in PBS (pH 7.4). Roots were washed for 1 h at RT under continuous shaking in 67 mM K_2HPO_4 (pH 12). The samples were then incubated for 1 h at RT under continuous shaking in an aniline blue solution composed of 0.01% aniline blue (w/v) in 67 mM K_2HPO_4 (pH 12). Roots were washed again for 1 h at RT under continuous shaking in 67 mM K_2HPO_4 (pH 12). Imaging was conducted with an excitation wavelength of 405 nm and emission detection from 490-510 nm.

Images were taken with a Leica TCS SP8 confocal microscope (Wetzlar, Germany). The percentage area of ConA staining was quantified using ImageJ[81] in maximum intensity projections of 10-slice Z-stacks with an image depth of 10 μm. At least 24 different root regions of each genotype were analyzed.

QUANTIFICATION AND STATISTICAL ANALYSES

All descriptions of the statistical analyses and statistical parameters can be found in the figure captions. A summary of the statistical analyses can be found in Table S3.